Final Report for
Supply and Services Canada
No. 23440-9-9002/01-SS

Pressure and Temperature Dependence of Interfacial Tensions and Contact Angles in Oil/Water and Bitumen/Water Systems

Principal Investigator: Dr. A.W. Neumann

March 1991

MICROMEDIA

University of Toronto
Department of Mechanical Engineering
5 King's College Road
Toronto, Ontario
M5S 1A4

82 pp

TABLE of CONTENTS

SCOPE AND OBJECTIVES 3

BACKGROUND & INTRODUCTION 4

AXISYMMETRIC DROP SHAPE ANALYSIS (ADSA) 9

MATERIALS 11

METHODS & APPARATUS 12
- Apparatus For Interfacial Tension and Contact Angle Measurements 12
- Density Measurements 13
  - i) Density Apparatus 15
  - ii) Experimental Procedure 16

RESULTS AND DISCUSSION 17
- Density Measurements of Alkanes 17
- Time Dependence of Interfacial Tension 19
  - i) At Ambient Conditions 19
  - ii) At Elevated Pressures 22
- Pressure Dependence of Interfacial Tension of Model System (Water-Hydrocarbon) 24
- Liquid-Liquid-Solid Contact Angle Measurements 28

SUMMARY OF CONCLUSIONS 34

BENEFITS TO EMR FROM THIS INVESTIGATION 36

PUBLICATIONS FROM RESEARCH PROJECT 37

FUTURE WORK 37

REFERENCES 38

APPENDIX A, B, C and D 39

SCOPE AND OBJECTIVES

Interfacial tension is one of the main parameters controlling oil recovery in most tertiary recovery schemes; similarly the contact angle that is formed at the intersection of the interfaces bounding the oil/water/rock phases play a crucial role in secondary recovery (water flooding). As the pressure in a reservoir is typically several hundred atmospheres and the temperature is typically 200°C the relevant interfacial tension and contact angle have to be measured under these conditions. In essence, previous experimental methodology has not been or could not be applied under these conditions. The Axisymmetric Drop Shape Analysis (ADSA) has been adopted to measurements under these conditions. We therefore planned to determine interfacial tensions as well as carry out a fundamental study of contact angle phenomena under realistic conditions with the view of elucidating its role in enhanced recoveries.

The objectives of this project thus were:

1) *Generation of fundamental understanding of pressure and temperature dependence of oil/water and bitumen/water interfacial tensions and contact angle phenomena.*

2) *Development of strategies to optimize the interfacial tension parameters for the purpose of enhanced oil and bitumen recovery.*

BACKGROUND & INTRODUCTION

In the long range a key point in the recovery of liquid and solid hydrocarbons will likely be the inability, even in the best of cases (i.e., the recovery of conventional crude), to recover more than approximately 30% of the reserves at the end of water flooding. In the more difficult situations, such as the recovery of bitumen from oil sands, the prospects are even poorer. There is obviously a considerable incentive and indeed need to develop tertiary recovery schemes in order to liberate more hydrocarbons from the reserves. A variety of such schemes has been suggested and in some cases implemented to a modest extent. Such strategies may be grouped into two categories, thermal flooding and chemical flooding. Examples of thermal flooding are *in situ* combustion, steam flooding and wet combustion; chemical flooding strategies include caustic flooding, surfactant flooding, micellar-polymer flooding and carbon dioxide flooding. It is safe to say that not all of these tertiary methods will prove to be economically viable, and some may pose considerable environmental threats.

But a common feature of most of these techniques is that a two phase hydrocarbon/water system is generated. At the onset of tertiary recovery, oil is believed to be trapped in the porous reservoir rock as discrete droplets, or "ganglia". Two forces act upon the so-called ganglion,

viscous forces and capillary forces. The ratio of these two forces, the so-called capillary number (*Nc*), is inversely proportional to the oil/water interfacial tension; at the end of secondary recovery this interfacial tension is typically 20 to 30 mJ/m^2. Under these conditions the viscous forces are overpowered by the capillary forces, which are responsible for trapping oil within the reservoir rock. A substantial reduction of the interfacial tension, by three or four orders of magnitude, is required to make *Nc* sufficiently large to facilitate flow. At these reduced interfacial tensions, the oil droplets are easily deformed and pass more easily through the narrow channels between sand grains. One of the difficulties connected with this problem is the fact that it is not necessarily correct to suggest that the smaller the interfacial tension, the better. A decrease in interfacial tension will enhance emulsification, rendering the oil droplets smaller and smaller. While such systems may flow very easily, they are very difficult to separate subsequently. Thus, it becomes apparent that in the solution of any practical problem in this area, an optimum interfacial tension needs to be established. Thus, the need arises to be able to measure, control and monitor the oil/water interfacial tension. There is a very significant road block preventing easy implementation of such a scheme: In a reservoir the ambient pressure is typically several hundred atmospheres and the ambient temperature is typically 200°C.

For secondary oil recovery one of the goals is to detach oil from the rock by displacing it with water, i.e., water flooding. In such a system a contact angle is formed at the intersection of the interfaces bounding the oil/water/rock phases. Hence, contact angle phenomena will play a crucial role during this enhanced recovery. The magnitude of the contact angle, i.e., the wettability, is not only governed by the interfacial tensions of the three phases but also by the physical properties of the solid surface. Real surfaces exhibit roughness and often considerable heterogeneity which prevent measurements of a unique contact angle: contact angle hysteresis is observed on these surfaces. The difficulty in determining wettability is the fact that contact angles and contact angle hysteresis can only be determined experimentally. Thus, not only do the interfacial tensions (oil/water, water/rock and rock/oil) need to be established, but a fundamental study of the contact angles as well as contact angle hysteresis at reservoir conditions must also be conducted.

In our opinion, only three interfacial tension methodologies may be applicable. Light scattering methods, the spinning drop technique and drop shape methods. Of those, the light scattering methods are the most recent. they depend on the fact that thermal effects tend to produce ripples on a quiescent liquid\fluid interface, while interfacial tension tends to keep the interface flat at all times. The size of the ripples, detectable by laser light

scattering, is therefore a measure of the interfacial tension. While it is claimed that interfacial tensions down to 10^{-5} mJ/m^2 can be measured with the technique, there is very little information on studies of liquid\liquid systems available.

The spinning drop technique, developed and implemented prior to development of the technique of the thermal ripples, has been the workhorse of the oil industry, although there are persistent reports from investigators who failed to obtain satisfactory results from the technique. The technique depends on a mathematically rigorous analysis inter-relating interfacial tension and shape parameters of a drop spinning at a given rate within a second liquid. The technique requires mechanical feed-throughs, which generate immense difficulties when one attempts to implement the technique at elevated temperatures and pressures. To the best of our knowledge, these difficulties have not been overcome so far.

The method to be used in this project is a static drop shape method. For present purposes, this technique has a decisive advantage over all other techniques: It is applicable to both pendent and sessile drops, and for the latter the output data comprise both of interfacial tension and contact angle. In general, the shape of a static drop is determined by gravity and interfacial tension. In the case of sessile drop, gravity tries to make the drop flat; this is opposed by interfacial tension, which tries to make the drop round. The deviation from spherical shape is a measure of the

interfacial tension. Until recently, only empirical drop shape methods were available. While theoretical approaches existed, they did not function satisfactorily, for a variety of reasons. Progress in these matters was made recently in our laboratory (Ph.D. theses of Y. Rotenberg, J.K. Spelt and P. Cheng) by the development of computer algorithms of a numerical integration of the Laplace equation of capillarity, i.e., the differential equation describing the shape of liquid\fluid interfaces. This technique for measuring interfacial tension is called Axisymmetric Drop Shape Analysis (ADSA) (see details below).

In yet another development a suitable high pressure, high temperature cell has been designed, built and tested in this laboratory. This cell allows for both pendent and sessile drop analysis for pressures up to 5000 psi and temperatures of up to 200°C.

During this contract period, three mechanical engineering students worked on this research project as their B.A.Sc. thesis. One of these students extended his Bachelors thesis topic to a M.A.Sc. thesis (in progress). Copies of the three B.A.Sc. theses are included in the Appendices B, C and D. One paper has been submitted for publication of work stemming from this research project (a copy is included in the Appendix). One other paper is in preparation and will be submitted for publication in the near future.

AXISYMMETRIC DROP SHAPE ANALYSIS (ADSA)

The method used for measuring interfacial tensions is a static drop method. In general, the shape of a static drop is determined by local gravity and interfacial tension. In the case of a pendent drop, gravity tries to elongate the drop while interfacial tension tends to make the drop spherical. In the case of a sessile drop, gravity tries to make the drop flat; this is opposed by interfacial tension, which tries to make the drop spherical. The deviation from spherical shape is a measure of the interfacial tension. Progress recently made in our laboratory allows the calculation of the interfacial tension by computer algorithms which integrates the Laplace equation of capillarity, i.e. the differential equation describing the shape of the liquid-fluid interface. The required input for the Axisymmetric Drop Shape Analysis is:

a) profiles of pendent or sessile drops,

b) the local gravity constant and

c) the density of the two measuring fluids.

The first input is obtained by a computer based imaging technique or image analysis. The gravity constant is measured locally by the Physics Department at the University of Toronto. The last required input, the density difference, has to be measured. Reliable density data for water and

air at elevated pressure and temperature are readily available. Literature values for the densities of hydrocarbon, crude oils or bitumen at elevated temperatures and pressures, however, are rare or non-existent. Thus, an independent method of measuring the densities of systems of interest has to be employed, and relatively high accuracy is required. The output from ADSA in case of the pendent drop is the interfacial tension, drop volume and surface area. For a sessile drop the output consists of the contact angle, θ, liquid-vapour surface tension, γ_{LV}, drop volume, radius of contact and surface area.

A block diagram of the experimental set-up for ADSA is illustrated in Figure 1. A high-resolution video scanner (Cohu 4800 CCD monochrome camera) is attached to a distortion free Wild Leitz Macroscope (Apozoom) which is used to focus on the drop image. Images of the pendent or sessile drop are transmitted to an ITI digitization board which performs the frame grabbing and digitization of the images. Subsequently the array of intensity levels is stored in memory of a Digital MicroVax II computer. Images are digitized to a 512 x 512 pixel array with 256 gray levels, where 0 represents black and 255 represents white. The computer performs the image analysis and computations. A precise finely ruled linear grid facilitates the detection of any distortion that may arise from the optics in both the horizontal and vertical direction. Coordinate points of the drop

profile are found using an edge detection scheme called the gradient magnitude method. This method encompasses the transformation of a gray level image to a gradient image. The pixels with the maximum gradient magnitude perpendicular to the drop profile are used as the input coordinates for ADSA. Figure 2 shows the image of a alkane pendent drop immersed in water as reproduced on a laser printer. Figure 3 is of a water sessile drop in alkane on a teflon (FEP) surface. Figure 4 shows the plot of the profile coordinates of the drop in Figure 2. These coordinate points are fitted with a theoretical Laplacian curve by the ADSA computer program.

MATERIALS

The n-alkanes used were n-hexane (C_6H_{14}) with a purity of 99.2%, n-heptane (C_7H_{16}), 99.8% pure, and n-decane ($C_{10}H_{22}$), 99.6% pure. All three were obtained from the Aldrich Chemical Company. The purity was determined by gas chromatography and reported by DeFilippis [1]. The density meter was calibrated using water and nitrogen. The water used was doubly distilled (ultra pure water which has been deionized) using the Sybron Barnstead NANOpure II still, and then degassed by placing it in a desiccator under vacuum for several hours until no more gas bubbles

formed. Nitrogen 99.997% pure in a 42 MPa (6000 psig) cylinder from Linde Union Carbide was also used. Density as a function of pressure for water and nitrogen can be found in references [2] and [3], respectively.

METHODS & APPARATUS

Apparatus For Interfacial Tension and Contact Angle Measurements

Figure 5 shows the experimental set-up for the pressure-temperature cell configuration. The cell depicted in this illustration is a first generation cell. The cell is a 316 stainless steel hollow cylinder with 1 inch thick optically flat pressure windows filled at each end. All lines and connections are pressure rated 316 stainless steel. The cell is transilluminated by white monochromatic light dispersed by a frosted glass plate. The pressure and the formation of the pendent drop is regulated with a HPLC pump. A Schaevitz pressure sensor (range 0 - 5000 psig) is used to measure the pressure. Two immersion heaters that run the length of the cell are used to heat the cell.

Details of a redesigned cell (second generation) are shown in Figures 6 and 7. Full details of this cell are contained in the B.A.Sc. Thesis of K.

Dehdashtian which is included in its entirety in Appendix D. This thesis constituted part of this project contract. Figure 6 is a cut-view, similar to the view in Figure 5 and Figure 7, showing the details of the centre block (side-view), i.e., the chamber in which the actual drops are formed. In the second generation cell, (details can be found in Appendix D) the main improvement is the design of the inside chamber. It can accommodate a flat solid substrate like a polymer, glass, quartz or compressed clay on which a sessile drop can be formed. For temperature control the cell is encompassed with a liquid double walled jacket connected to a thermostated water or oil bath. It has been designed for temperatures up to 200 °C. Thus, contact angle phenomena as a function of temperature and pressure can be studied with this cell.

Density Measurements

An Anton Paar DMA 40 digital density and external DMA 512 cell was used to measure the density of alkanes, crude oils and bitumen. This apparatus allows the accurate measurement of the density of liquids and gases at elevated pressures and temperatures. Densities can be measured with an accuracy of 1×10^{-4} g/cm^3 at pressures of up to 400 atmospheres

and temperatures of up to 150°C.

The density meter works on the principle that the period of oscillation, T, (which the density meter measures) of a vibrating U-tube depends on the density of the sample contained in the U-tube. An equation can be written relating the period of oscillation to the density of the sample, the volume, mass and spring constant of the U-tube. Rearranging this equation and grouping the terms which are constants produces a formula which relates ρ to T and two constants A and B. Therefore, if the densities of two substances are known, and the T-values measured, the equation can be solved for the calibration constants A and B using equations (1) and (2).

$$A = \frac{T_1^2 - T_2^2}{\rho_1 - \rho_2} \tag{1}$$

$$B = T_1^2 - A\rho_1 \tag{2}$$

where 1 represents water and 2 nitrogen. These constants will be valid under the conditions of temperature and pressure for which the calibration procedure was conducted. Knowing A and B, the density of any fluid under these given conditions can be found by equation (3), where T is the measured period of oscillation of the fluid [4,5,6].

$$\rho = \frac{T^2 - B}{A} \tag{3}$$

With this equipment we are able to measure accurately the density of any liquid to be used for interfacial tension studies at elevated temperatures

and pressures. We can acquire a very accurate measure of density at any desired condition thus allowing accurate interfacial tension measurements.

i) Density Apparatus

Figure 8 is a schematic of the experimental set-up used for the density measurement of the n-alkanes. In the calibration procedure there are two modifications of the set up as diagramed. The first is that the intermediate cell is not used, thus line 3 connects directly to the density meter. The second modification is relevant for the nitrogen run only; during this run the pump is replaced by the nitrogen bottle. Because it is not desirable for the pump (Eldex AA-100-S) to be used to pump hydrocarbons (since the pump would have to be cleaned after each use), an intermediate cell is used (which can be readily cleaned). The hydrocarbons are less dense than water and also insoluble. Thus, they float on top of the water, and when the pump is run, the water acts like a piston which pushes the hydrocarbon into the density meter. The fittings used to withstand these pressures are made of stainless steel and were either self-sealing (Swagelok) or wrapped with Teflon tape (Cajon). Schaevitz pressure transducer number P1021-0005 which is accurate to ±5 psi (±0.03 MPa) was used with

an Aries Instruments indicator type 8142-000-00. A "J" thermocouple was used with an indicator made by Thermo Electric model 3164101111 which has a digital readout good to ±0.1°C. The water bath was a MGW Lauda C 12 model B-1.

ii) Experimental Procedure

The temperature of the density meter was controlled by a water bath. The thermocouple was inserted into the density meter before the experiment, to find the proper setting for the water bath. The thermocouple was later placed in the water bath to monitor its temperature. The n-alkane experiments are basically the same as the calibration experiments (done with water and nitrogen), except for the differences already mentioned. The system is set up as in Figure 8, and the density meter is allowed to come to thermal equilibrium with the water bath. The T-value is then recorded and the pressure is increased. The density meter is again allowed time to reach thermal equilibrium (which is indicated by T coming to a steady value) before T is recorded. The pressure is again increased, the fluid allowed to come to equilibrium, and T is recorded. This procedure is then repeated until the maximum pressure has been reached. The pressure is then released, and the U-tube cleaned with an appropriate solvent; acetone was used, and the U-tube dried with air using the built in pump.

RESULTS AND DISCUSSION

Density Measurements of Alkanes

The pressure coefficient of the interfacial tension, $\delta\gamma/\delta P$, has been shown theoretically to be related to the thickness of the interfacial region between the liquids [1,7,8]. It has also been shown that the pressure coefficient of the interfacial tension is a measure of the distance between the two Gibbs dividing surfaces of zero mass. The magnitude of $\delta\gamma/\delta P$, or the distance between the two surfaces of zero mass can be expected to be of the order of 0.1 nm or less. Since, experimentally, interfacial tensions can be measured with our set-up only at pressures up to a few hundred atmospheres, the change in interfacial tension over this range will only be 1 to 2 mJ/m^2. Thus, it is quite obvious that very accurate interfacial tension measurements are needed in order to observe the small change over a given pressure range. The interfacial tension is directly related to the density difference between the two fluids. Thus, the densities of the fluids (alkanes, water, crude oils, bitumen, etc.) must also be known with great accuracy.

As already discussed, the density values at elevated pressures of liquids of interest are not available in the literature. Pressure dependence of the density of three alkanes, decane, hexane and heptane has been measured

using the digital density meter.

Two sets of density measurements were performed. In the first set of measurements a 50 psi interval was chosen for measurements ranging from 0 to 5000 psig. A total of 100 data points for this pressure range were obtained. This turned out to be too small of an interval to work with. The limiting factor for the measuring interval is the resolution of the digital density meter. The change in density due to an increase of 50 psi is smaller than the resolution of this particular density meter. In the second set of measurements the pressure interval was chosen at 100 psi. The density increase with this pressure interval was larger than the resolution of the density meter. Next, the results and analysis of the latter investigation will be presented.

The experimental results are given in Figure 9 and in Table I. Fifty data points (represented by the dots in this figure) were obtained for each of the three n-alkanes. The Tait equation, of the form given by Eqn. (4), was chosen to fit the data and is represented by the curve drawn in Figure 9.

$$\frac{\rho - \rho_0}{\rho} = C \log \left[\frac{B + p}{B + p_0} \right] \qquad (4)$$

This equation has been frequently used to fit p-ρ data for compressed liquids and is known to reproduce reliably density data at high pressures [9]. This form of the Tait equation (using log to the base 10) relates density ρ at

pressure p to the density ρ_0 at atmospheric pressure p_0 and the parameters B and C. Eqn. 4 was fit to the data for each n-alkane and B and C were then optimized. Details of the optimization process can be found in reference [10][1]. The optimized B and C values for the three alkanes are given in Table II. Included in the table are comparison values between the data and the Tait equation (Eqn. 4).

The measured density data of the three alkanes can be well represented by the Tait equation from 0 to 5000 psi. The experimental error in the p-ρ has been estimated to be 0.02%. The Tait parameters for each of the n-alkanes was optimized using 50 data points on the 21.2°C isotherm.

Time Dependence of Interfacial Tension

i) At Ambient Conditions

In our initial investigation of hydrocarbon-water interfacial tensions (alkanes, benzene and steam and fire flooded bitumen) it has been established that the interfacial tension decreases over time, reaching a steady state value after approximately 6 minutes [1]. An example of a time

[1] Also included in Appendix A.

dependence result of decane in water at ambient conditions is shown in Figure 10 and of steam flooded bitumen in Figure 11. Regular distilled water was used and two grades of alkanes; a commercial grade from Aldrich of at least 99.2% purity or better and an API SRM grade of at least 99.96% purity or better. In all cases the interfacial tension of the Aldrich hydrocarbon-water systems dropped at a considerably faster rate than the interfacial tension of the API SRM hydrocarbon-water systems. These phenomena were attributed to impurities present in both water and hydrocarbon as well as to contaminants from the experimental apparatus. In general, impurities tend to migrate to the interface of a system and cause a decrease in the interfacial tension. As a consequence of this phenomenon, sufficient time must be allowed before performing any pressure dependent measurements to allow the interfacial tension to reach a steady state value.

Such time dependence studies have been repeated with the commercial alkanes, but with a better grade of distilled water and a more stringent cleaning procedure of the apparatus and the associated hardware (Details of the cleaning procedure will be detailed in S.S. Susnars M.A.Sc. thesis). The water was distilled using a Corning MEGA-PURE distiller with an added Sybron/Barnstead Nanopure II filtration unit. Two time dependent measurements were performed with decane. First the dynamic behaviour of a decane pendent drop in water and next a water pendent drop

in decane was analyzed. The resulting time dependent behaviour for both systems is presented in Figure 12. Identical surface tension and dynamic behaviour is observed for both systems. Thus, the measured interfacial tension is invariant to the liquid-liquid configuration, as it should be. Consistency in the measured interfacial tensions for both configurations affirms the correctness of the interfacial tension measurement for liquid-liquid systems.

The time dependence of the interfacial tension has been plotted as a function of the inverse of the square root of time in Figure 13. A linear dependence would imply that the time dependence may be due to diffusion of surface active impurities from the two bulk phases to the interface. Both curves reveal a linear decrease. A correlation coefficient of $r = -0.99$ has been calculated for both cases. Therefore, the small decrease in the interfacial tension over time is most likely due to impurities present in the commercial alkane or contaminants present in the apparatus.

The total decrease in the interfacial tension for this particular system is only 0.4 mJ/m^2, which is significantly lower than what was measured previously, suggesting higher purity of the system. The dynamic behaviour of the interfacial tension seems to be a consequence of impurities or more precisely contaminants diffusing from the bulk fluids to the interface. Thus, for real systems of oil and bitumen, detailed studies of the dynamic

behaviour of the interfacial tension must be made at each state before pressure and temperature investigations can be carried out. More important, detailed studies of the time dependence of the interfacial tension at elevated pressures and temperatures are required before results of $d\gamma/dP$ are correctly interpreted.

ii) At Elevated Pressures

In this experiment time dependent studies were conducted at various pressures with decane in double distilled water. Eleven different pressures, ranging from 0 to 5200 psig were investigated. At each pressure, the interfacial tension was monitored over a 20 minute interval.

Figures 14 to 24 show the time dependent results for the eleven different pressures. At ambient conditions, the interfacial tension appears to have reached a steady state in about 1 to 2 minutes. These results are identical to the results presented in Figure 12. This trend is observed for pressures up to 2585 psig. However, at the higher pressures there is a much greater decrease in the interfacial tension over the 20 minute time interval. In fact γ appears not to have reached steady state at all. It is believed that the reason for this change in the time dependent behaviour of

the interfacial tension is due to air present in the system. Although the water was degassed prior to the experiment, there are always small air pockets in the cell and bubbles in the tubes which will be added to the bulk fluid during the initial set-up. When compressed, the air dissolves in the bulk water, then by diffusion and convection (pumping water into the cell to increase the pressure) this dissolved air migrates to the interface and decreases the interfacial tension.

It might also be suggested that part of the decrease in γ at higher pressures might be due to pressure loss occurring during the 20 minute time interval. The interfacial tension results presented in all these figures is for a density difference value recorded at the beginning of the time dependence study, i.e., at time zero. There is, however, a small loss in pressure over time at the elevated pressures. This is not due to any leaks in the system, but most likely the O ring groves are getting filled with fluid over time. The pressure loss at each of the pressure is presented in Table III. At the highest pressure of 5177 psig, the pressure dropped by 259 psi over the 20 minute time interval. To correct for the pressure loss the interfacial tension was recalculated using the actual density value. The calculations were carried out for the highest pressure only. The results are plotted in Figure 25. This figure reveals that the loss in pressure has a very small impact on the time dependence of pressure at the elevated pressures. Hence, such

small pressure losses cannot be attributed to such large decreases observed in the interfacial tension with time.

These results complicate the interpretation of pressure dependence of interfacial tension. If the interfacial tension reached a steady state value at all pressures, then the steady state values would be used to compare γ at each pressure. Since the above results reveal that this is not possible, a different strategy was developed. Details are presented in the next section.

Pressure Dependence of Interfacial Tension of Model System (Water-Hydrocarbon)

Prior to the present study we had investigated the pressure dependence of the interfacial tension of alkanes and benzene [1]. Interfacial tensions were measured at eight to ten different pressures ranging from 0 to 5000 psi. In all systems studied a linear increase in the interfacial tension was observed with an increase in pressure. The slopes, confidence limits and regression coefficients were determined for all systems. In all cases, the slopes and regression coefficients were found to be significant at the 99% confidence level. All the results, however, revealed small dips in the interfacial tension at approximately 68 and 200 atms. Similar dips were

observed in the density plots.

In the present study we address the non-linear trends in the pressure dependence in the interfacial tension to clarify whether these dips are indeed a real physical effect. First a more detailed study of the density of hydrocarbons at elevated pressures was performed. Details of density measurements were discussed earlier in this report. Also, different curves were fitted to the density vs. pressure results. Pressure dependence of the interfacial tension was then interpreted in terms of the different density curves (see below for details). Furthermore, twice as many interfacial tension measurements were made in the same pressure range. In analyzing these results the time dependence results discussed above were incorporated in establishing $d\gamma/dP$.

The pressure dependence of γ is plotted in Figure 26 for time t=0. An increase in γ is observed with increase in pressure. Also plotted are the results at t = 1200 seconds in Figure 27. Here the interfacial tension decreases with pressure. Since these points are not at steady state, as was observed in the time dependence study, this curve can not be readily interpreted. Only the first six points are at steady state and the rest are not. Further analysis was carried out with results at t = 0 seconds.

In performing the experiment, the drops at the higher pressures were formed over an extended time periods. That is, a new drop was formed

after the time study was completed at the last pressure. Then the pressure in the cell was slowly increased to the next pressure. This took anywhere from 10 to 20 minutes. Such large time spans are required to prevent drops being blown off from the needle. At the lowest pressures the drops are formed almost instantaneously. Therefore, at the lower pressures, the t=0 second values of γ will not be the same as the γ at t=0 seconds for the other higher pressures. Since γ reached a steady state in less than 2 minutes for the first two drops the γ at steady state was used for these drops as a better approximations to the t=0 second values used for the last 9 drops. Figure 28 shows the γ-P curve if this approximation is made.

A statistical analysis carried out on the data presented in Figure 26 and 28 showed that the third last data point was an outlier [10]. This point was rejected as an outlier with a 99% confidence limit. Using only 10 points, with the first two points at t=1200 seconds and the latter points at t=0 seconds, a linear regression was performed to establish the pressure dependence of interfacial tension. The data points together with the best straight line fit to the data are shown in Figure 29. The slope of the line, the intercept and the regression coefficient are presented in Table IV.

The results obtained for the pressure dependence of the interfacial tension are compared with literature values in Table V. The present $d\gamma/dP$ value is lower than those obtained in the literature. There are a number of

possible explanations for this difference. The interfacial tension is directly related to the density difference between the two liquids. It will be shown that $d\gamma/dP$ is strongly dependent on the density difference values used.

The density measurements performed at elevated pressures were fitted by the Tait equation (Eqn. 4). This equation was found to be the best representation of the density of n-alkanes versus pressure. Besides the Tait equation, a number of different equations can be fitted to the experimental density-pressure data points. The following equations were also fitted to the density-pressure data of decane:

1) $\rho = a_0$

2) $\rho = a_0 + a_1 P$

3) $\rho = a_0 + a_1 P + a_2 P^2$, and

4) $\rho = a_0 + a_1 P + a_2 P^2 + a_3 P^3$

where P is the pressure and ρ is the density. Also, in case of the straight line, case 2, the slope, a_1 was varied by:

5) 5% (a_1 + 5% a_1) and

6) -1% (a_1 + -1% a_1).

The density difference was then calculated using the density values calculated from the above fitted curves and literature density values of water. The density difference was then used as input to ADSA to calculate γ at elevated pressures from the acquired images of pendent drops. γ

results at elevated pressured for the above six cases are plotted in Figure 30. Using the data in this Figure, the $d\gamma/dP$ was calculated for the different density-pressure curve approximations. These results are presented in Table VI. It can be seen in Figure 30 that the calculated interfacial tension at elevated pressures is strongly dependent on the value of the density difference. More important, the slope of $d\gamma/dP$ is also strongly affected. Table VI also contains the calculated regression coefficient, r, for $d\gamma/dP$ calculations for the different density approximations. The largest r value, i.e., best linear fit, is obtained for the Tait equation fit to the density data.

The required input for ADSA is the density difference. Here, the density of the alkane is treated as the unknown and the density of water as known. For any other system, the density of both phases have to be known with the same accuracy in order to get accurate measurements of the interfacial tension, not only at elevated pressures but for all experimental conditions.

Liquid-Liquid-Solid Contact Angle Measurements

A detailed study of bitumen and crude oil contact angle phenomena at reservoir conditions can be undertaken only if a suitable model of the

reservoir rock is made. We proposed to use initially glass and/or quartz for the study of water-oil-solid contact angles and contact angle hysteresis. Before we attempted to work with the proposed system we have initiated a contact angle feasibility study with polymers. A water-hydrocarbon-Teflon system was chosen to establish ADSA for liquid-liquid-solid contact angle measurements and then establish a protocol for reservoir simulation systems.

First a time dependence study of liquid-liquid-solid contact angles was carried out, at ambient conditions. These experiments were carried out not in the temperature-pressure cell but in a clean quartz cuvette. This particular apparatus was chosen so as to eliminate any possibility of contamination. Although a stringent cleaning procedure is followed for the cell, there are many valves, pipes, connecting joints and a pump which could all be a source of contaminants during the actual experiment. The quartz cuvette was first cleaned by soaking in chromic acid for 24 hours and then rinsed and sonicated with distilled water and finally dried under a heat lamp. The Teflon (FEP) substrate was heat pressed against a finely ground and polished quartz glass slide slightly below its glass transition temperature [11]. This procedure produced a very smooth surface which is a prerequisite for any contact angle studies. The Teflon substrate was placed on the bottom of the cuvette and the cuvette was filled with decane. A drop of water was deposited on the substrate with a micrometer syringe.

An example of the sessile drop of water in decane on Teflon was given in Figure 3. Images of the drop were first taken right after the drop was formed and subsequently every 20 seconds for the first 2 minutes and then every 200 seconds for up to 20 minutes. The images of the sessile drops were analyzed by ADSA providing information on the time dependence of the radius of contact, the drop volume, the contact angle and the liquid-liquid surface tension. It was observed that the four measured parameters are constant over time as illustrated in Figure 31 to 34, respectively. The error bars in these figures represent 95% confidence limits. The average contact angle is 154° for this system and the mean water-decane interfacial tension is 49.9 mJ/m^2. This value for the interfacial tension compares well with the value obtained from pendent drop analysis. The steady state, or plateau value obtained from pendent drops of water in decane and decane in water is approximately 51.2 mJ/m^2 which is only 1.3 mJ/m^2 higher than this value. It is our experience that the interfacial tensions measured by ADSA from pendent drops are more accurate than from sessile drops [12]. The details will not be discussed here, but the differences have been attributed to imperfections of the solid surfaces. For practical purposes, we conclude that the interfacial tensions measured for the two configurations, sessile and pendent drops, are in good agreement. There was, however, no time dependence observed in the interfacial tension for the sessile drop. This is

further supported by the measured constant radius of contact diameter, drop volume and contact angle. This leads us to conclude that the time dependence experienced with the pendent drop in the cell is driven by impurities or contaminants present in the system.

An attempt was also made to study the behaviour of an alkane sessile drop in distilled water. This is the more practical method of measuring liquid-liquid-solid contact angles in particular for real oil or bitumen systems. For real systems, it is not possible to observe the water drop in bitumen or oil due to the opaqueness of both oil and bitumen. For the model alkane-water system, it is feasible, and more desirable, to observe alkane drops in water, because the cost of pure alkanes is high. In this case a relatively small amount of liquid is needed to form a sessile drop. Since the densities of hydrocarbons are lower than water an inverted drop method is used for this configuration. That is, the hydrocarbon drop in water is formed on a substrate from below. A decane drop in distilled water formed on the Teflon substrate is presented in Figure 35. For a hydrocarbon drop in water on Teflon a smaller contact angle is expected than for the water in hydrocarbon system. The contact angle for this configuration and the contact angle for the inverted system, water in hydrocarbon, should add up to 180°. For the drop presented in Figure 35, the contact angle is roughly 20°. The measured water in alkane contact angle is 154° which when

added to the above contact angle is equal to approximately 180°, as expected.

For this experiment we experienced some difficulties in analyzing the decane in water contact angles with ADSA. It seems that the alkane drop deviates slightly from a true sessile drop shape. This can be observed at the right and left side of the drop where there is a small inflection in the drop profile. In addition, the automated image analysis segment of ADSA requires that a reflection of the sessile drop be observed in the acquired picture. Using the reflection the exact location of the solid is calculated. Experimentally, the microscope is slightly tilted downwards in order to capture the reflection of the sessile drop. For liquid-liquid-solid sessile drops in the pressure cell, the reflection of the drop is experimentally harder to obtain. Reflections of small contact angles are harder to observe under normal conditions than for larger contact angles (see Figures 35 and 3). For this reason the decane was replaced with heptane, which formed a contact angle slightly larger than 90° in water on Teflon. For this case the reflection was observed and images of sessile drops at elevated pressures were analyzed by ADSA.

Results of contact angles measured at 8 pressures, ranging from 200 to 1650 psi are presented in Figure 36. A best straight line fit to the data is also drawn in this Figure. These results reveal an increase of 1.5° in the

liquid-liquid-solid contact angle with an increase in pressure of 1650 psi.

The above results are preliminary, to best of our knowledge we report here the first results of pressure dependence of contact angles. Several investigators have studied pressure dependance of γ but we haven't found any evidence in the literature of contact angles at elevated pressures. Our feasibility study has pinpointed major experimental difficulties in measuring contact angles under pressure. The difficulties have been identified and solutions for most of them have been worked on. Details of these solutions can be found in the B.A.Sc. thesis of M. Amani [13] (see Appendix C).

SUMMARY OF CONCLUSIONS

1) The densities of three pure alkanes, decane, hexane and heptane, were measured at pressures ranging from 0 to 5000 psi to an accuracy of $\pm 1 \times 10^{-4}$ g/cm^3. The Tait equation was found to provide the best fit to the data.

2) An improved pressure cell (second generation) was designed, built and tested allowing for pendent and sessile drop formation. The cell was designed for working pressures ranging from 0 to 5000 psi and temperatures as high as 200°C.

3) Axisymmetric Drop Shape Analysis (ADSA) was adopted to measure interfacial tension and contact angles at elevated pressures in the pressure cell.

4) Interfacial tension was measured of an oil-water and water-oil system. Both systems revealed identical γ and dynamic behaviour. The measured γ is invariant to the liquid-liquid configuration.

5) Time dependence studies show that at low pressures the interfacial tension of pure alkane and water systems reaches steady state within a short time. A small decrease in the interfacial tension was shown to be diffusion controlled. Small amounts of impurities present in the liquid-liquid system migrate to the interface, manifesting themselves in a slight decrease in γ. At the higher pressures there is a strong dependence in the interfacial tension on time. A large decrease in γ was observed in 20 minutes; in this time frame the interfacial tension did not reach steady state.

6) Calculation of interfacial tensions from the shapes of sessile or pendent drops requires as an input parameter the density difference between the two fluid phases. It has been show that the interfacial tension and its pressure dependence, $d\gamma/dP$ is very sensitive to the correctness of the density difference value used.

7) The $d\gamma/dP$ of decane-water was calculated to be 19.7×10^{-12} m. The increase in the interfacial tension over 5000 psi is only 0.75 mJ/m^2.

8) Pressure dependence of liquid-liquid-solid contact angles has been measured over a pressure ranging from 0 to 1600 psi. Over this pressure range, heptane-water-Teflon contact angle increased by only 1.5°.

BENEFITS TO EMR FROM THIS INVESTIGATION

The interfacial tension is one of the main parameters controlling oil recovery in most enhanced recovery schemes. The interfacial tension of a model system, pure alkane in water, was investigated at elevated pressures. Pressures ranging from 0 to 5000 psi were investigated, simulating reservoir conditions. A detailed study of the factors influencing the interfacial tension at elevated pressures of an ideal, pure system was undertaken with a view of elucidating the behaviour of crude oils and bitumens. It was established that the pressure dependence on the interfacial tension is quite small for a pure system. This may not be so for mixtures, surfactant systems, crude oils and bitumens. With the knowledge obtained for the pure system at elevated pressures, a systematic study can now be undertaken for crude oils and bitumens.

PUBLICATIONS FROM RESEARCH PROJECT

As stated in the research proposal two publications derived from this research will be published in the open literature. One paper deals with the density of alkanes vs. pressure. The title of this paper is: The Pressure Dependence of Density for n-Alkanes". The authors are: S.S. Susnar, C.J. Budziak, H.A. Hamza and A.W. Neumann. This paper has been submitted for publication in the International Journal of Thermophysics.

A second paper is in preparation. It will report the pressure dependence of interfacial tensions of liquid-liquid systems. This paper will be submitted for publication in the Journal of Colloid and Interface Science.

FUTURE WORK

Extension of this study to surfactants added to a two component system.

REFERENCES

1. F. DeFilippis, M.A.Sc. Thesis, U. of Toronto, Canada, 1989.

2. L. Haar, J. S. Gallagher, and G. S. Kell, NBS/NRC Steam Tables, (Hemisphere Publishing Corporation, New York, 1984).

3. B. A. Younglove, Thermophysical Properties of Fluids 1. Argon, Ethylene, Parahydrogen, Nitrogen, Nitrogentetrafluoride, and Oxygen., (J. Phys. Chem. Ref. Data **11** American Chemical Society and The American Institute of Physics, 1982).

4. Instruction Manual External Measuring Cell, DMA, (Anton Paar, Graz, Austria).

5. O. Kratky, H. Leopold, and H. Stabinger, Calculating Digital Density Meter for Liquids and Gases Instruction Manual, DMA 45, (Anton Paar, Graz, Austria).

6. Density and Related Values, DMA, (Anton Paar, Graz, Austria).

7. R.S. Hanson, J. Phys. Chem., **66**, 410, 1962.

8. R.J. Good, J. Colloid Interface Sci., **85**, 128, 1982.

9. J. H. Dymond, and R. Malhotra, Int. J. Thermophys., **9** 941 (1988).

10. S.S. Susnar, M.A.Sc. Thesis, U. of Toronto, (in preparation).

11. C.J. Budziak, Ph.D. Thesis, U. of Toronto, Canada, (in preparation).

12. P. Cheng, Ph.D. Thesis, U. of Toronto, Canada, 1990.

13. M. Amani, B.A.Sc. Thesis, U. of Toronto, 1991.

14. K. Motomura, H. Iyota, M. Aratono, M. Yamanaka, and R. Matuura, J. Colloid Interface Sci., **93**, 264 (1983).

15. H.Y. Jennings Jr. J. Colloid Interface Sci., **24**, 323 (1967).

TABLE I: Pressure-density data for Aldrich n-hexane, n-heptane, and n-decane.

PRESSURE		DENSITY		
		HEXANE	HEPTANE	DECANE
(psig)	(MPa)		(kgm^{-3})	
0	0.10	658.92	682.68	728.91
100	0.79	659.70	683.41	729.48
200	1.48	660.47	684.12	730.05
300	2.17	661.24	684.83	730.62
400	2.86	662.00	685.53	731.19
500	3.55	662.76	686.23	731.75
600	4.24	663.51	686.92	732.31
700	4.93	664.26	687.60	732.87
800	5.62	665.00	688.28	733.43
900	6.31	665.74	688.95	733.98
1000	7.00	666.48	689.63	734.54
1100	7.69	667.20	690.29	735.09
1200	8.38	667.93	690.94	735.64
1300	9.07	668.65	691.59	736.18
1400	9.75	669.36	692.24	736.72
1500	10.44	670.00	692.82	737.20
1600	11.13	670.62	693.38	737.68
1700	11.82	671.26	693.96	738.17
1800	12.51	671.93	694.56	738.68
1900	13.20	672.60	695.16	739.19
2000	13.89	673.30	695.80	739.73
2100	14.58	674.02	696.45	740.30
2200	15.27	674.67	697.04	740.80
2300	15.96	675.20	697.50	741.20
2400	16.65	675.74	698.00	741.62
2500	17.34	676.32	698.51	742.06

TABLE I: Pressure-density data for Aldrich n-hexane, n-heptane, and n-decane continued.

PRESSURE		DENSITY		
		HEXANE	HEPTANE	DECANE
(psig)	(MPa)		(kg/m^{-3})	
2600	18.03	676.92	699.05	742.53
2700	18.72	677.55	699.63	743.03
2800	19.41	678.22	700.23	743.55
2900	20.10	678.87	700.83	744.06
3000	20.79	679.31	701.22	744.40
3100	21.48	679.78	701.65	744.77
3200	22.16	680.28	702.10	745.16
3300	22.85	680.82	702.60	745.59
3400	23.54	681.40	703.12	746.05
3500	24.23	682.01	703.69	746.53
3600	24.92	682.66	704.29	747.05
3700	25.61	683.09	704.68	747.38
3800	26.30	683.51	705.07	747.72
3900	26.99	683.98	705.50	748.09
4000	27.68	684.48	705.98	748.49
4100	28.37	685.03	706.49	748.93
4200	29.06	685.61	707.04	749.40
4300	29.75	686.23	707.63	749.90
4400	30.44	686.71	708.08	750.28
4500	31.13	687.12	708.48	750.61
4600	31.82	687.57	708.91	750.97
4700	32.51	688.05	709.38	751.36
4800	33.20	688.58	709.89	751.79
4900	33.89	689.14	710.44	752.25
5000	34.58	689.75	711.03	752.74

TABLE II: Parameters for the Tait equation.

n-alkane	B (MPa)	C	ρ_o (kgm^{-3})	σ (kgm^{-3})	Max. dev. (kgm^{-3})
Hexane	40.065	0.1655	658.9	0.097	0.26
Heptane	40.745	0.1484	682.7	0.094	0.17
Decane	52.735	0.1444	728.9	0.071	0.19

where $\sigma = \left[\frac{1}{n}\sum_{1}^{n}\left(\rho_{expt} - \rho_{calc}\right)^2\right]^{1/2}$ and Maximum deviation = $|\rho_{expt} - \rho_{calc}|$

TABLE III: Intial and final pressures during the time dependence at elevated pressures experiments for decane in water.

PRESSURE RUN	INTIAL PRESSURE (time = 0 s)	FINAL PRESSURE (time = 1200 s)	ΔP
(psig)	(psig)	(psig)	(psig)
0	30	29	1
1	32	31	1
2	592	500	92
3	947	831	116
4	1995	1839	156
5	2585	2431	154
6	3000	2775	225
7	3528	3308	220
8	3900	3680	220
9	4456	4216	240
10	5177	4918	259

TABLE IV: Linear regression results of pressure dependence of the interfacial tension of decane in water.

m	b	r
($mJ/m^2 bara \times 10^{-3}$)	mJ/m^2	
1.97	51.276	0.992

where the equation of the line is given by:

$$\gamma = m P + b$$

and r is the linear correlation coefficient ($r = \pm 1$ is a perfect linear fit, and $r = 0$ is no linear fit at all). The pressure is in bars absolute and the interfacial tension is given in mJ/m^2.

TABLE V: Comparison of $\left[\frac{\partial \gamma}{\partial P}\right]_T$ -values for decane with literature values.

$\left[\frac{\partial \gamma}{\partial P}\right]_T$ ($\times 10^{-12}$m)	95% C.L.	TEMP (°C)	SOURCE
19.7	2.0	21	PRESENT STUDY
42.6	10	21	DEFILIPPIS API SRM [1]
46.4	9	21	DEFILIPPIS ALDRICH [1]
29.6	---	25	MOTOMURA [14]
27.0	---	25	JENNINGS [15]

Table VI: Effect of $\Delta\rho$ on $\left[\frac{\partial\gamma}{\partial P}\right]_T$ -values for decane.

$\left[\frac{\partial\gamma}{\partial P}\right]_T$ ($\times 10^{-12}$m)	r	$\Delta\rho$ USED
19.7	0.992	WATER DATA-TAIT EQN
69.4	0.991	$\Delta\rho$=CONSTANT
20.1	0.900	1ST ORDER
17.6	0.871	1ST ORDER ε=+5%
20.5	0.905	1ST ORDER ε=-1%
19.1	0.970	2ND ORDER
18.5	0.976	3RD ORDER

Note that r is the linear correlation coefficient.

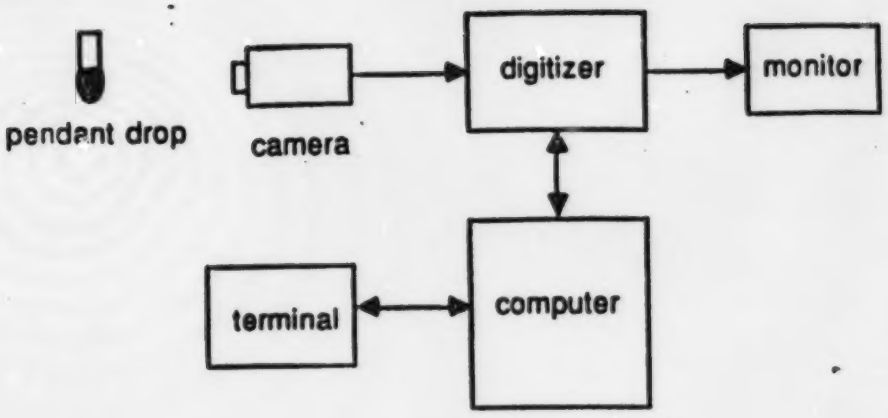

Figure 1: Block diagram of Drop Image Analysis set-up.

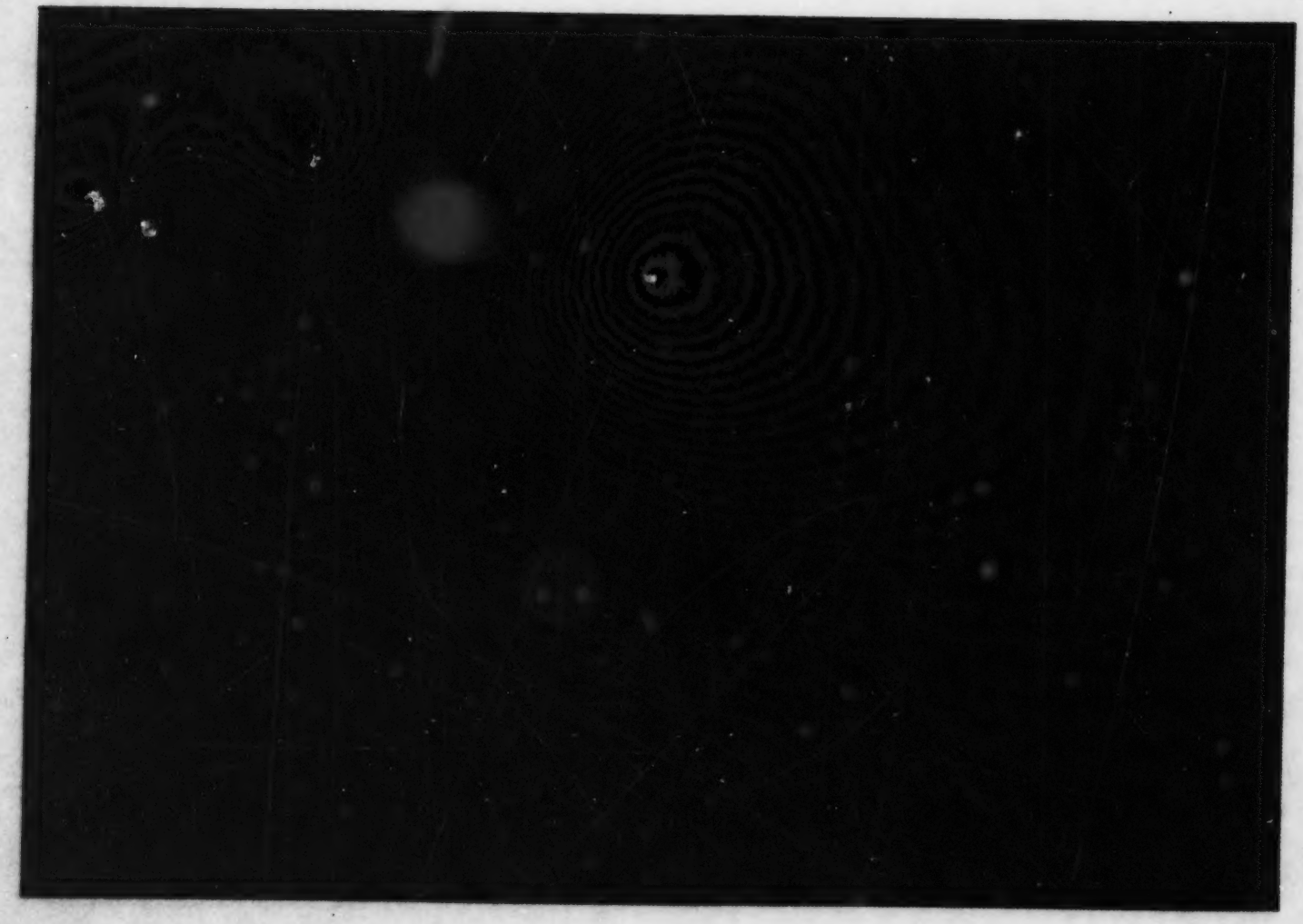

Figure 2: Laser printer reproduced image of an alkane drop immersed in water.

Figure 3: Laser printer reproduced image of an alkane sessile drop in water on a Teflon (FEP) substrate.

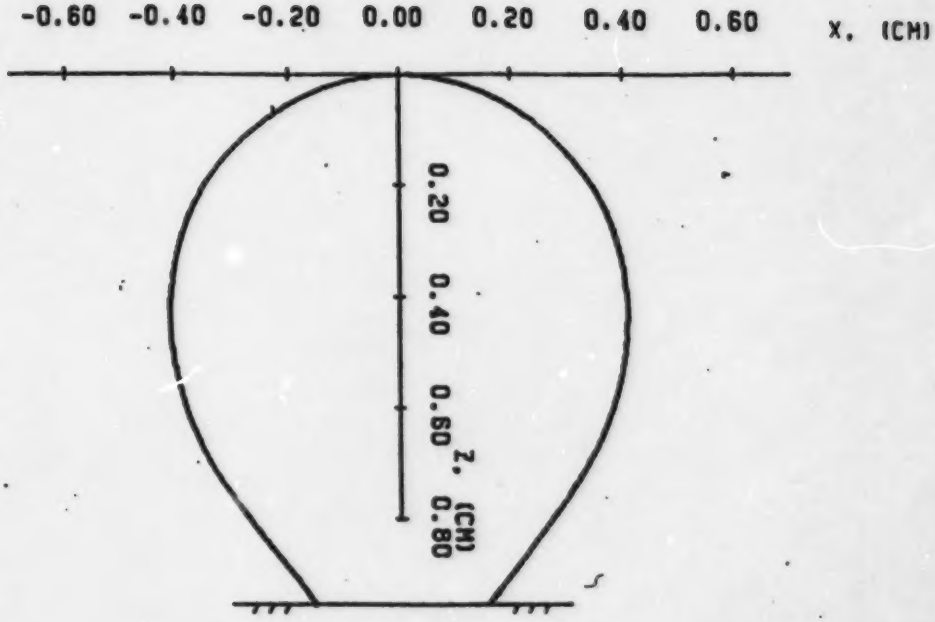

Figure 4: Profile coordinates of pendent drop of Figure 2 fitted with a theoretical Laplacian curve.

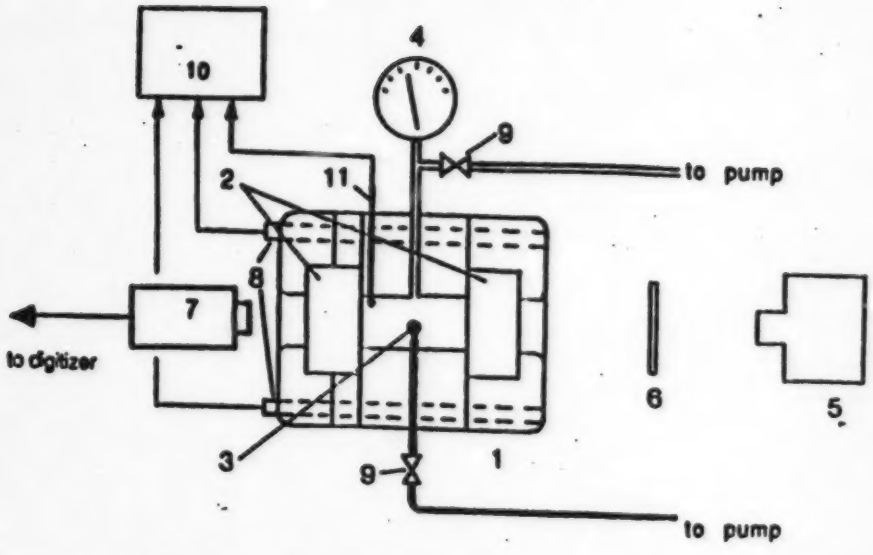

Figure 5: Pressure/temperature cell apparatus set-up.

1. pressure/temperature cell
2. optical glass windows
3. pendant drop
4. pressure gauge
5. light source
6. diffuser
7. camera
8. immersion heaters
9. isolation valves
10. temperature programmer
11. thermocouple

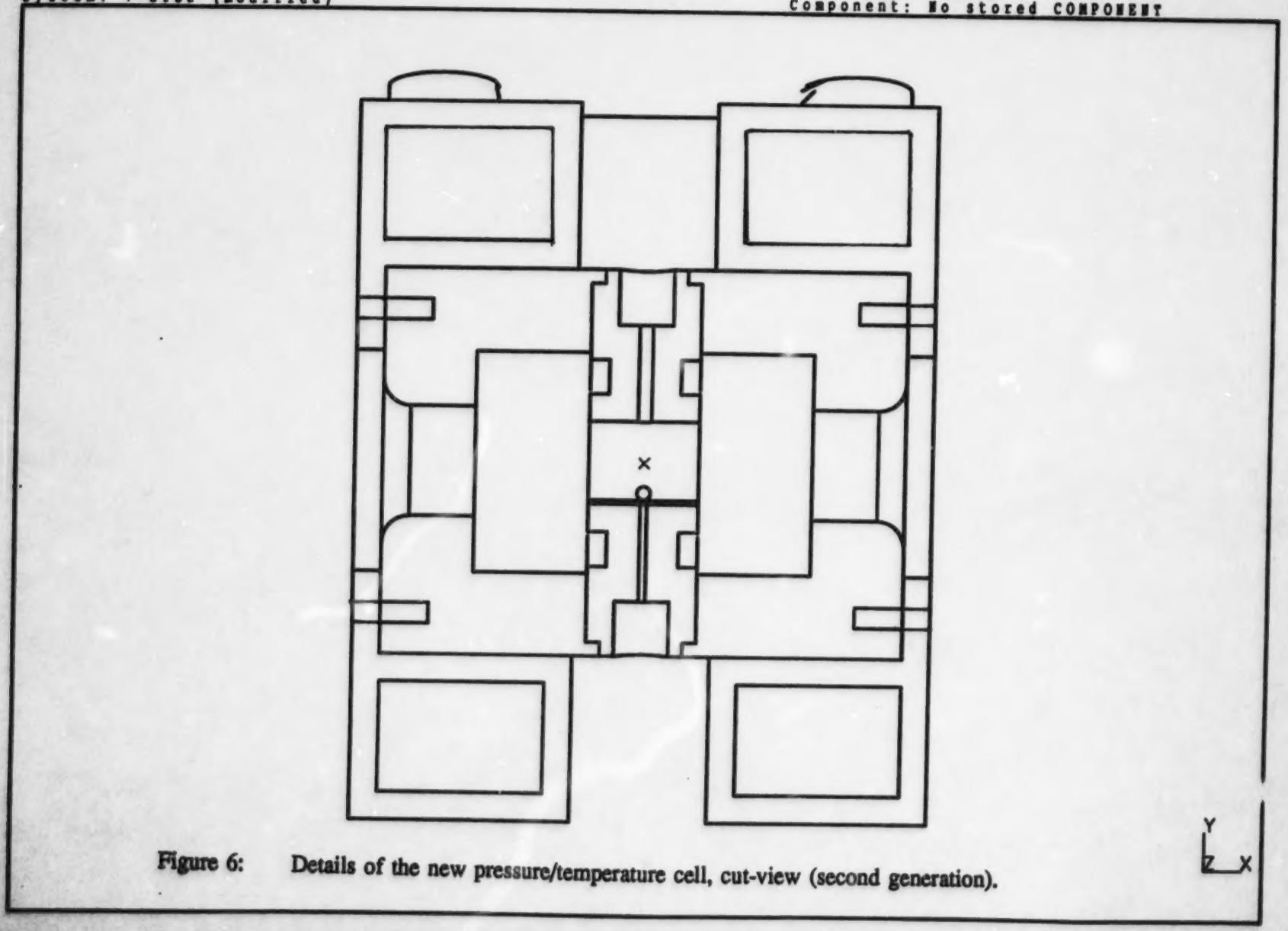

Figure 6: Details of the new pressure/temperature cell, cut-view (second generation).

SDRC I-DEAS 3.8: Object Modeling 21-Sep-89 16:36:27

DATABASE: RIGHT FLANGE
VIEW:No stored VIEW
Task: OBJECT
Object: 5-BODY

UNITS = IN
DISPLAY:No stored OPTION
Bin: 1-MAIN

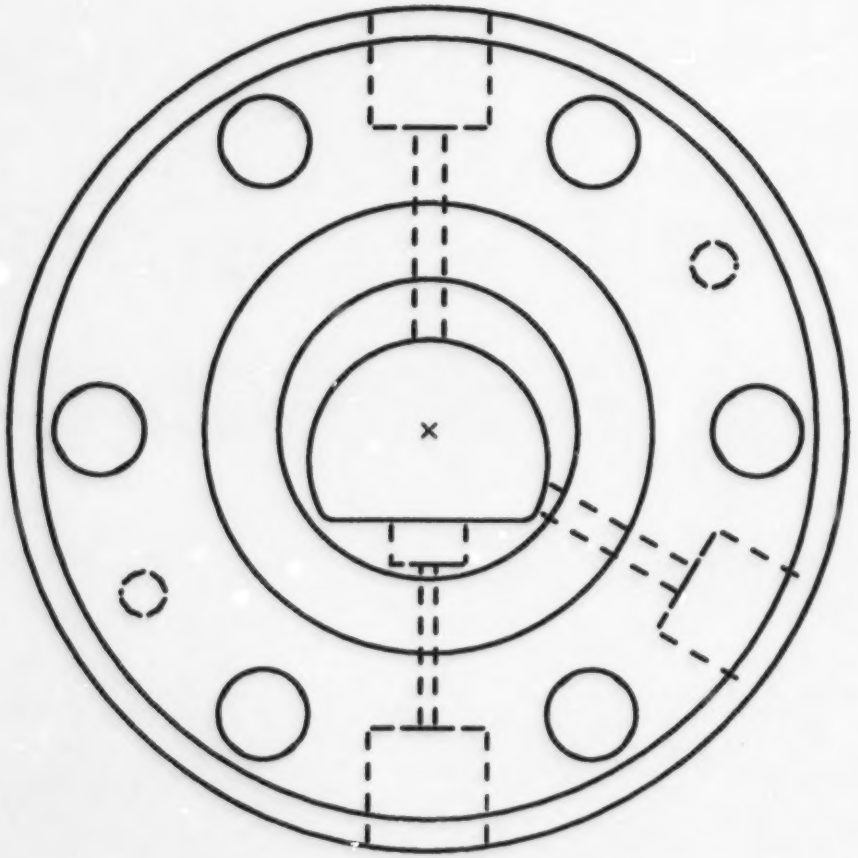

Figure 7: Side-view of the centre block of the new pressure/temperature cell.

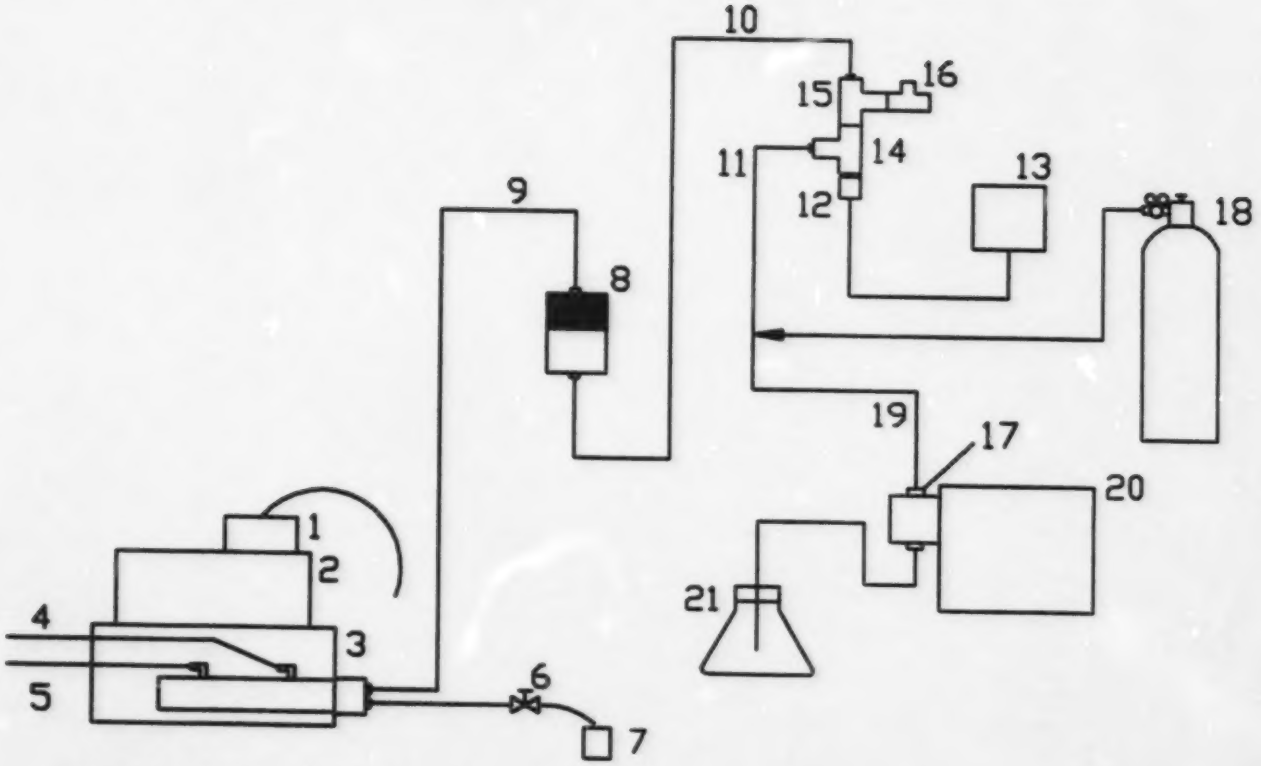

Figure 8: The density experiment apparatus.

1. Thermocouple
2. DMA 45
3. DMA 512
4. From water bath
5. To water bath
6. Discharge valve
7. Beaker for the discharge
8. Intermediate cell filled with alkane
9. Line 2
10. Line 3
11. Line 1
12. Pressure Transducer
13. Display for Pressure Transducer
14. Street Tee
15. Tee
16. Relief valve
17. Pressure connector
18. Nitrogen bottle
19. 316 Stainless steel pressure tubing
20. Pump
21. Flask of doubly distilled water

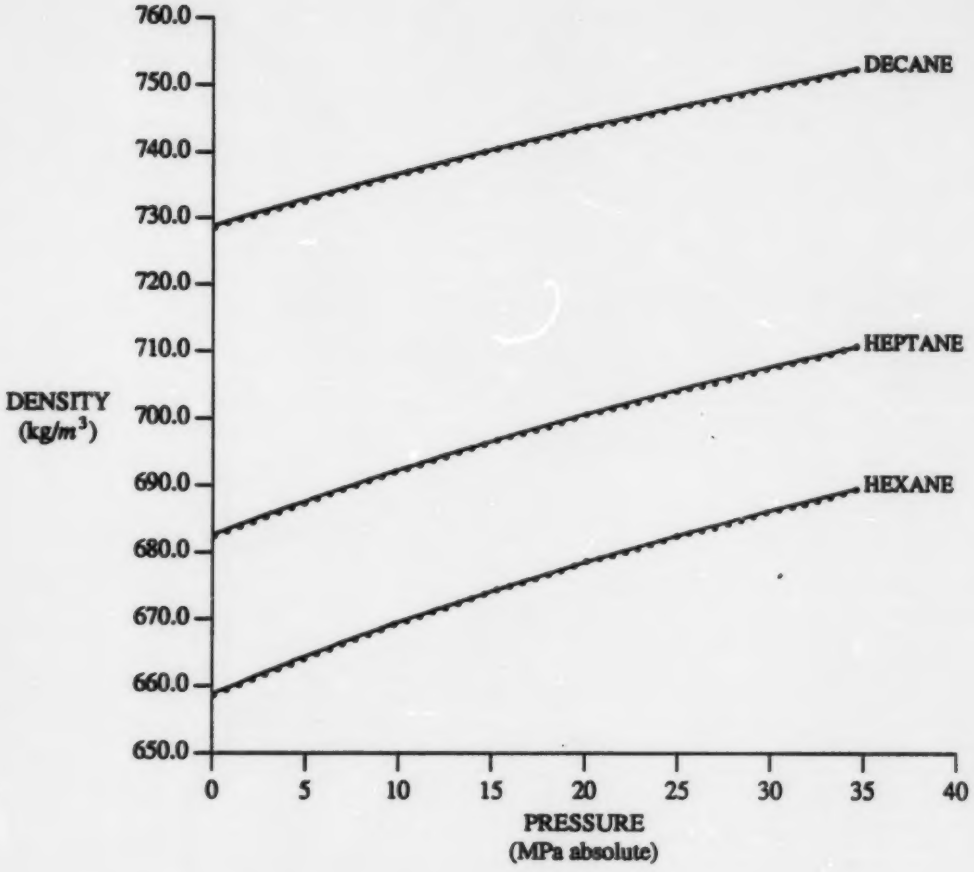

FIGURE 9: Density (kgm^{-3}) versus pressure (MPa absolute) for Aldrich n-hexane (99.2%), n-heptane (99.8%) and n-decane (99.6%) at 21.2 °C. The data are represented by the Tait equation.

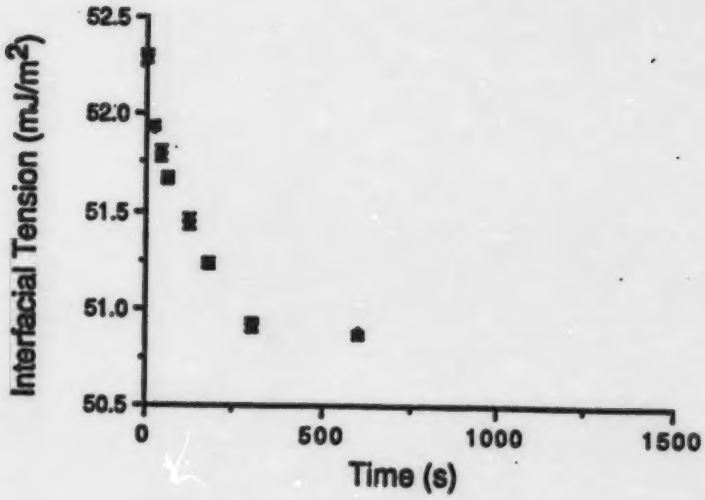

Figure 10: Interfacial tension versus time for Aldrich decane-water system at ambient conditions.

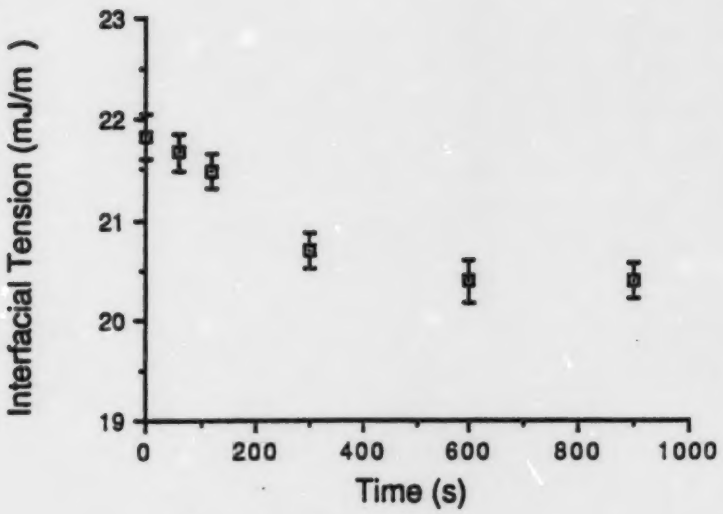

Figure 11: Interfacial tension versus time for steamflood bitumen-water system.

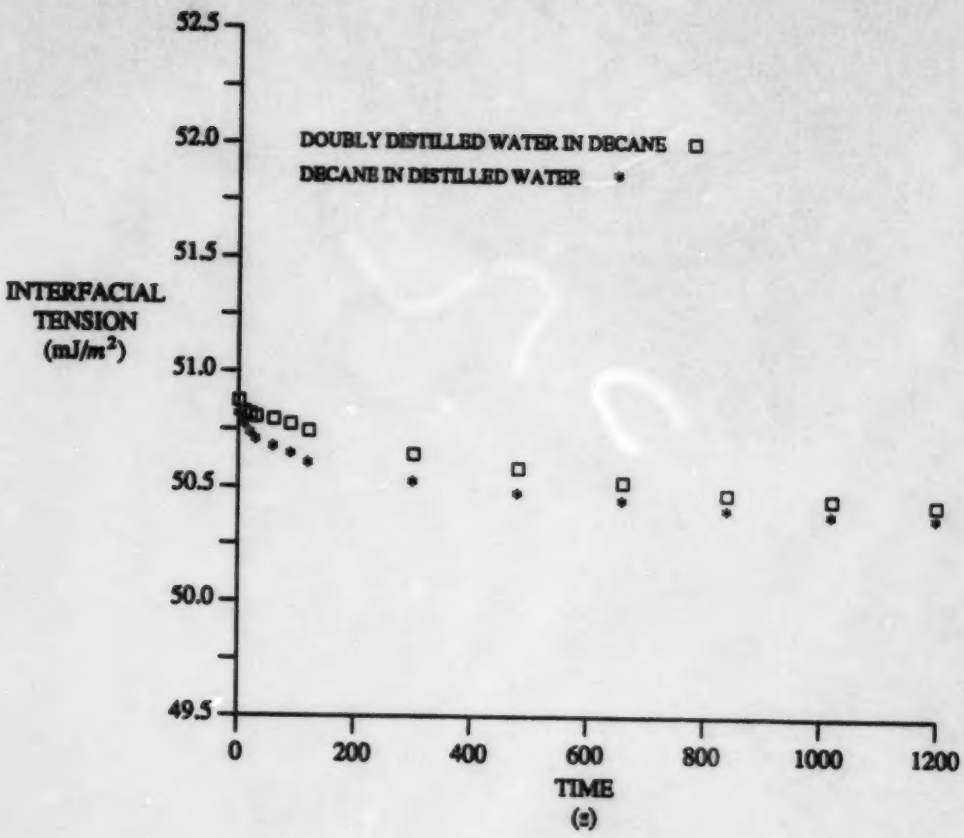

Figure 12: Interfacial tension (mJ/m^2) versus time (s) for doubly distilled water in decane and decane in distilled water.

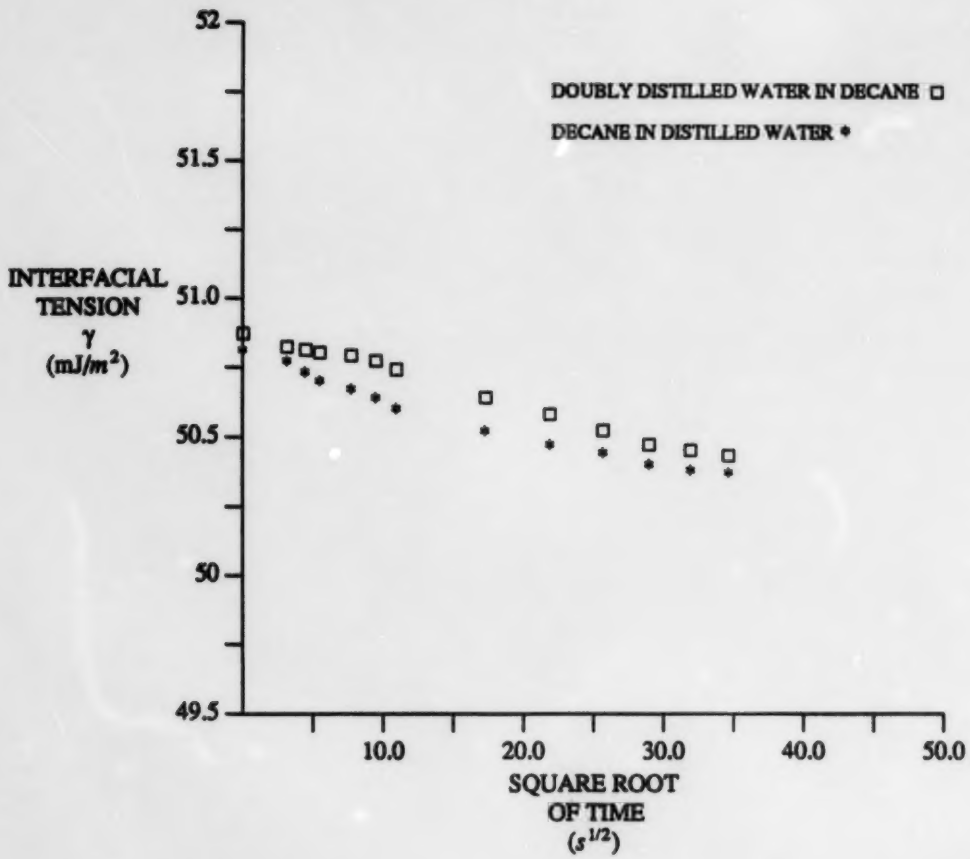

Figure 13: Interfacial tension (mJ/m^2) versus the square root of time ($s^{1/2}$) for doubly distilled water in decane and decane in distilled water.
Decane in distilled water has a correlation coefficient of $r = -0.986$.
Doubly distilled water in decane with a correlation coefficient of $r = -0.997$.

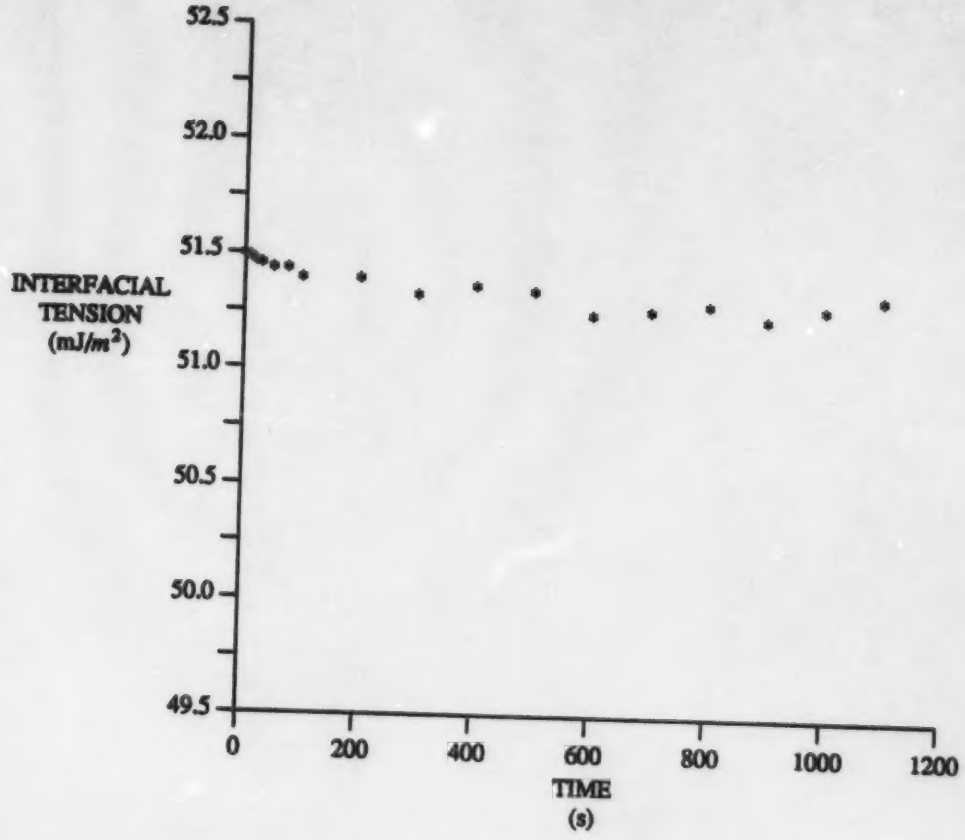

Figure 14: Interfacial tension (mJ/m^2) versus time (s) for decane in degassed doubly distilled water at pressure 30 psig.

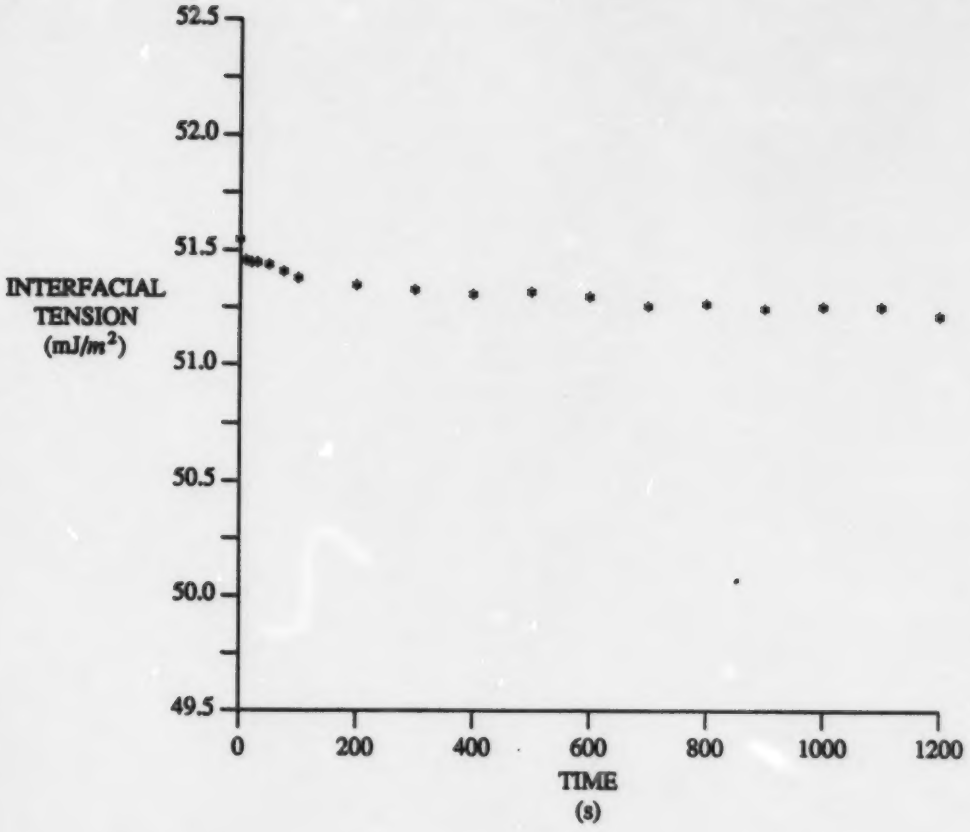

Figure 15: Interfacial tension (mJ/m^2) versus time (s) for decane in degassed doubly distilled water at pressure 32 psig.

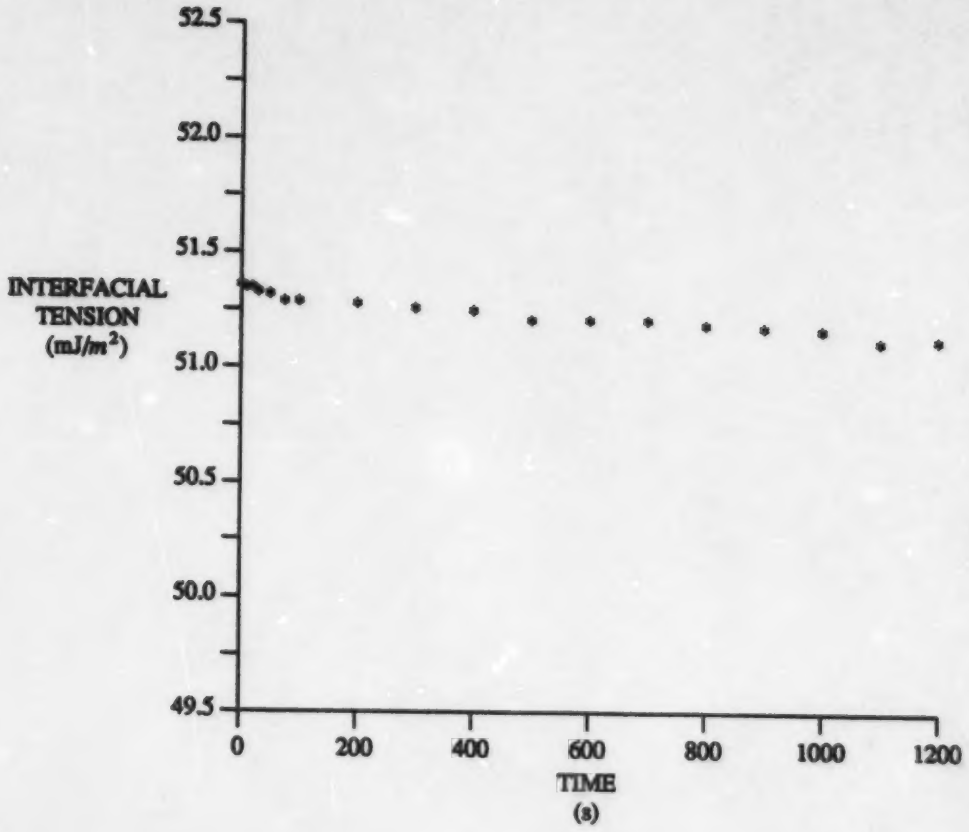

Figure 16: Interfacial tension (mJ/m^2) versus time (s) for decane in degassed doubly distilled water at pressure 592 psig.

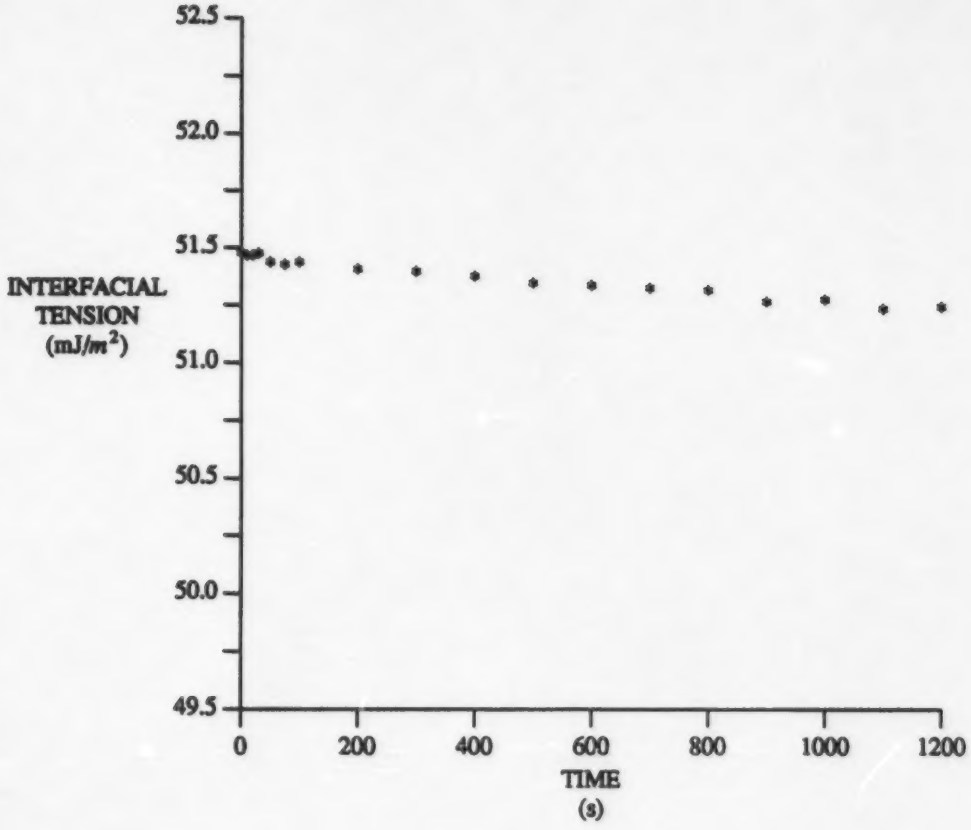

Figure 17: Interfacial tension (mJ/m^2) versus time (s) for decane in degassed doubly distilled water at pressure 947 psig.

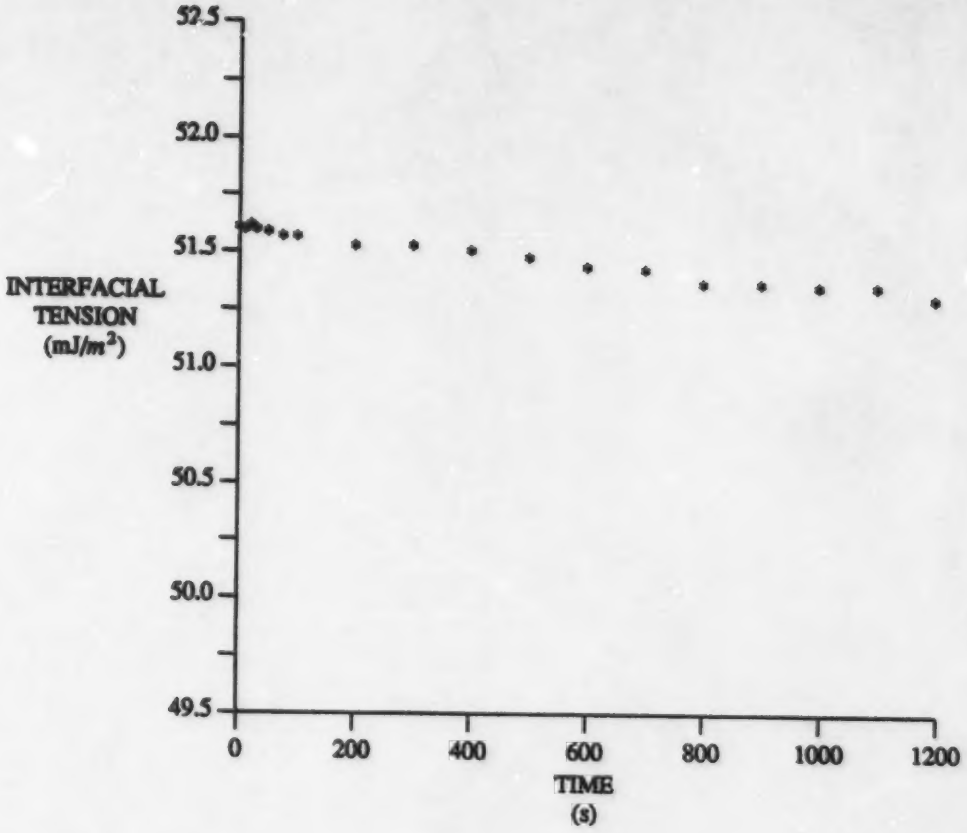

Figure 18: Interfacial tension (mJ/m^2) versus time (s) for decane in degassed doubly distilled water at pressure 1995 psig.

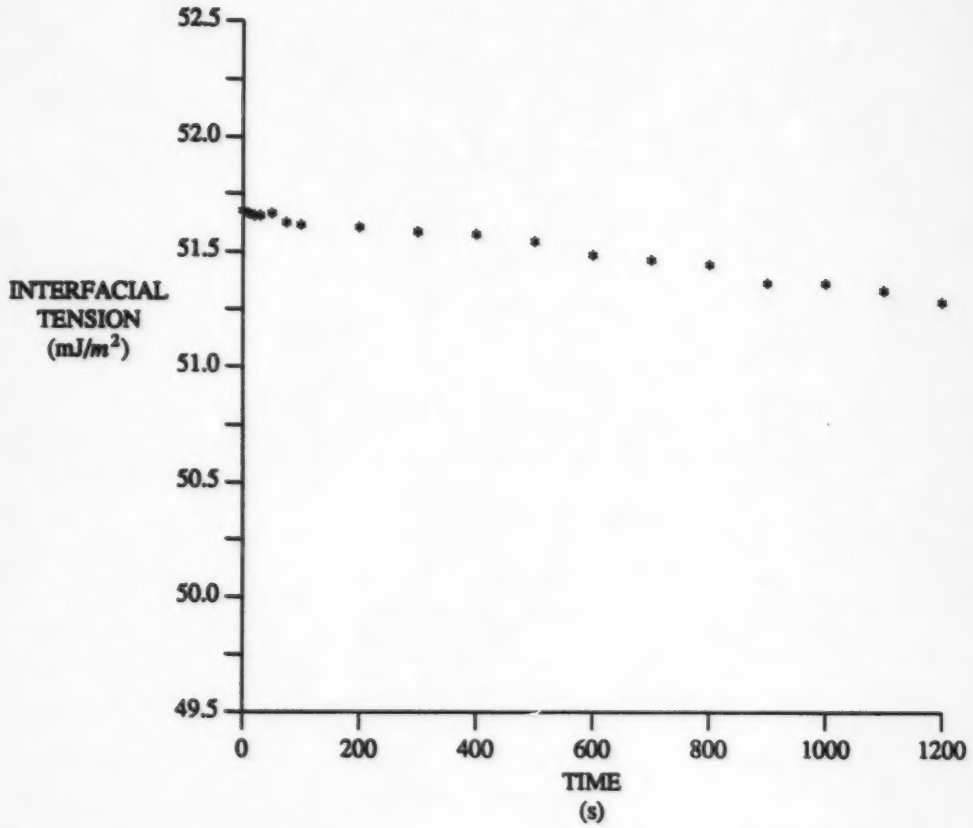

Figure 19: Interfacial tension (mJ/m^2) versus time (s) for decane in degassed doubly distilled water at pressure 2585 psig.

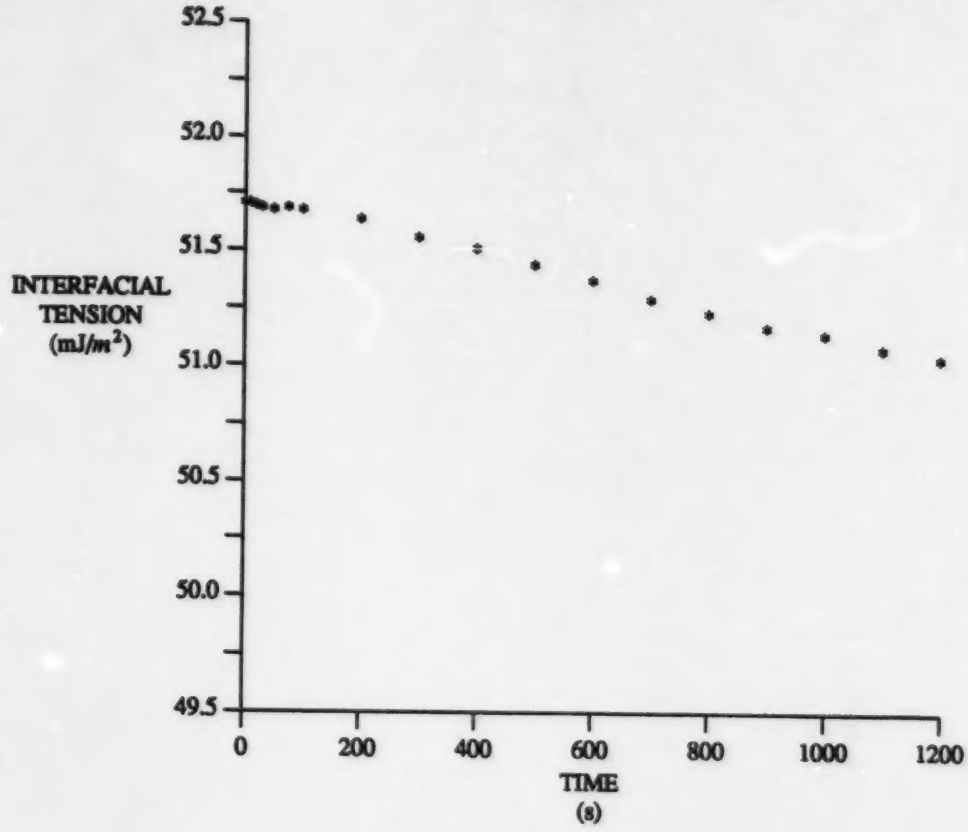

Figure 20: Interfacial tension (mJ/m^2) versus time (s) for decane in degassed doubly distilled water at pressure 3000 psig.

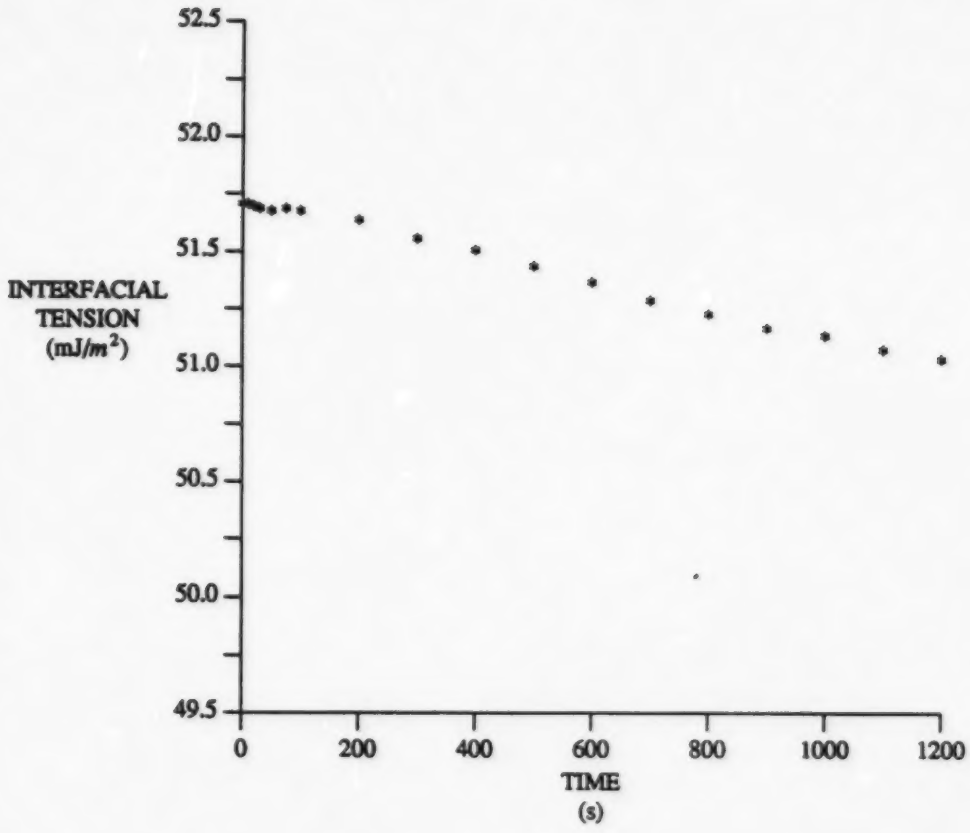

Figure 20: Interfacial tension (mJ/m^2) versus time (s) for decane in degassed doubly distilled water at pressure 3000 psig.

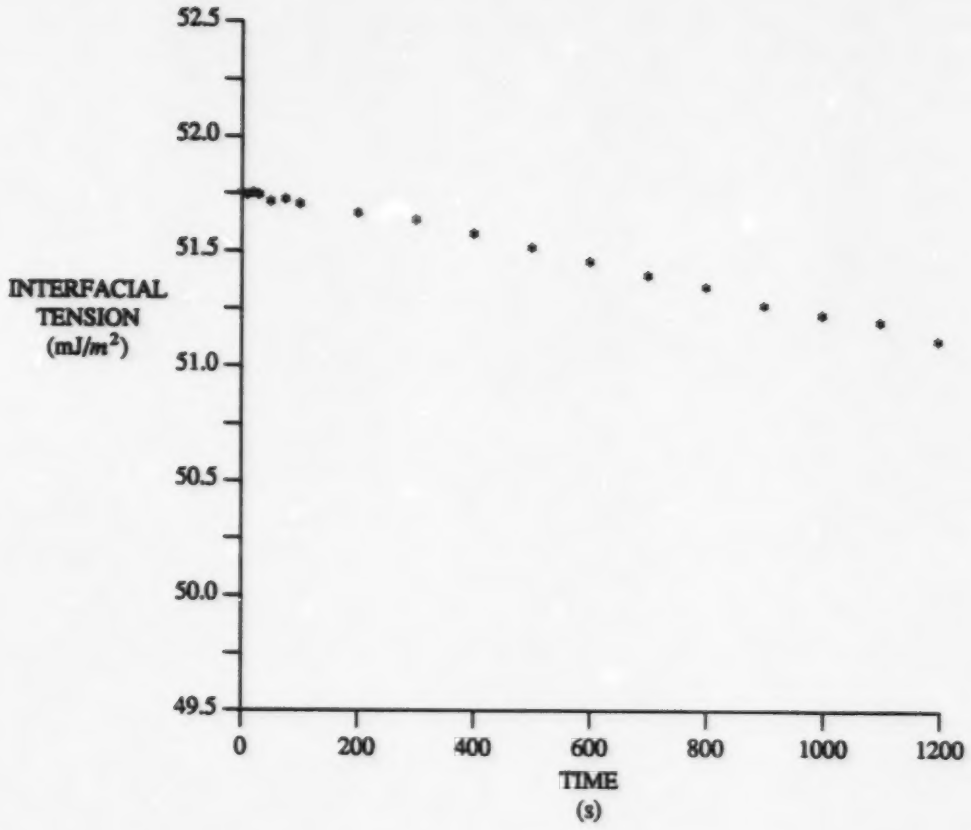

Figure 21: Interfacial tension (mJ/m^2) versus time (s) for decane in degassed doubly distilled water at pressure 3578 psig.

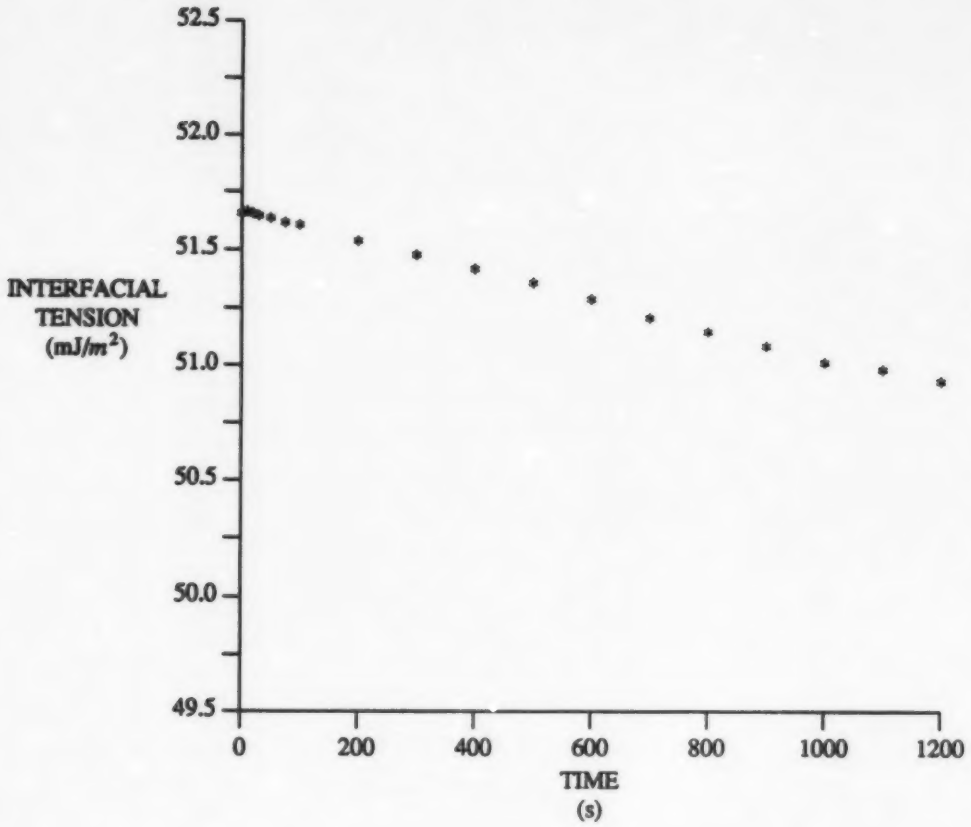

Figure 22: Interfacial tension (mJ/m^2) versus time (s) for decane in degassed doubly distilled water at pressure 3900 psig.

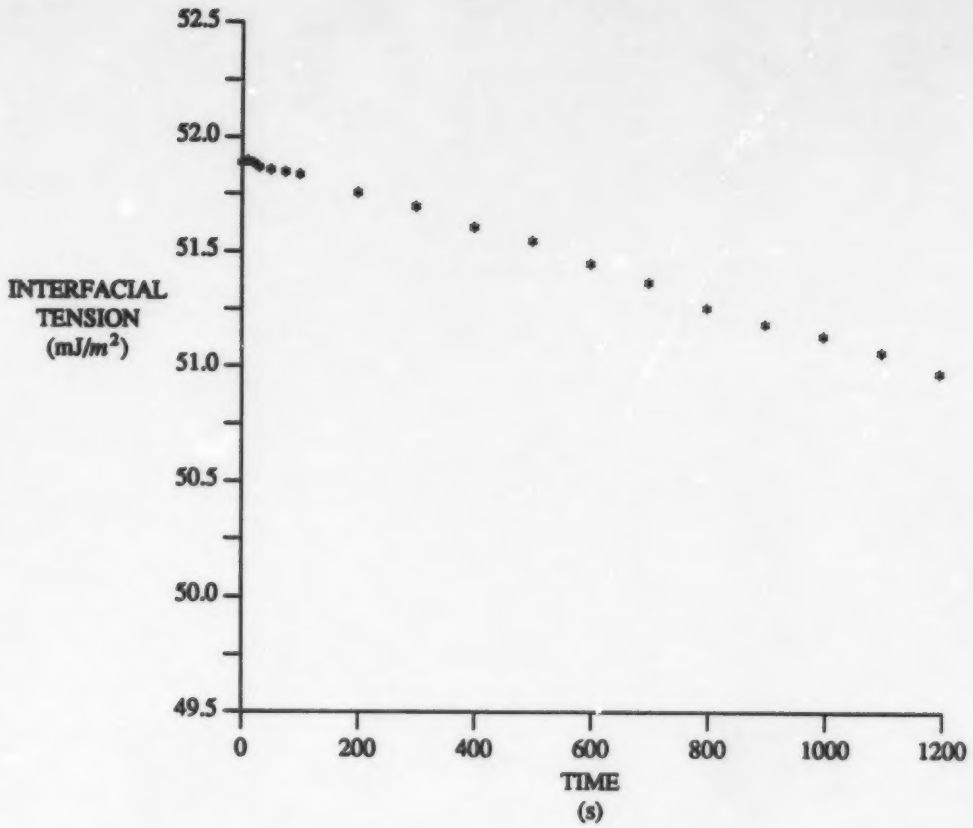

Figure 23: Interfacial tension (mJ/m^2) versus time (s) for decane in degassed doubly distilled water at pressure 4456 psig.

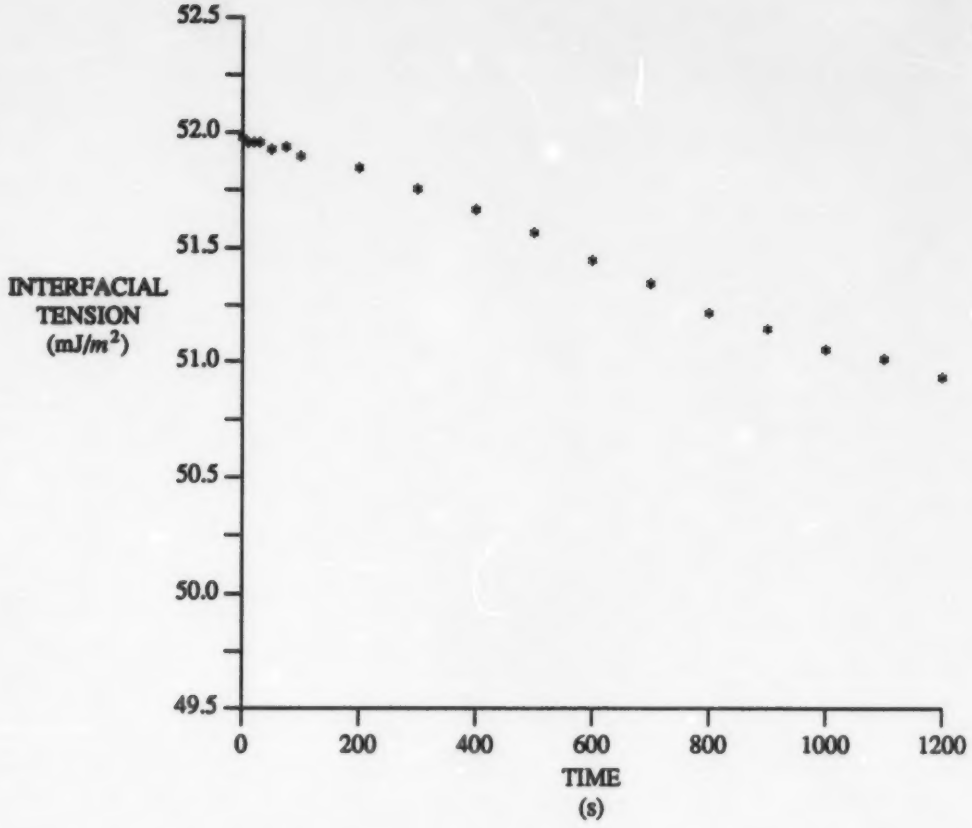

Figure 24: Interfacial tension (mJ/m^2) versus time (s) for decane in degassed doubly distilled water at pressure 5177 psig.

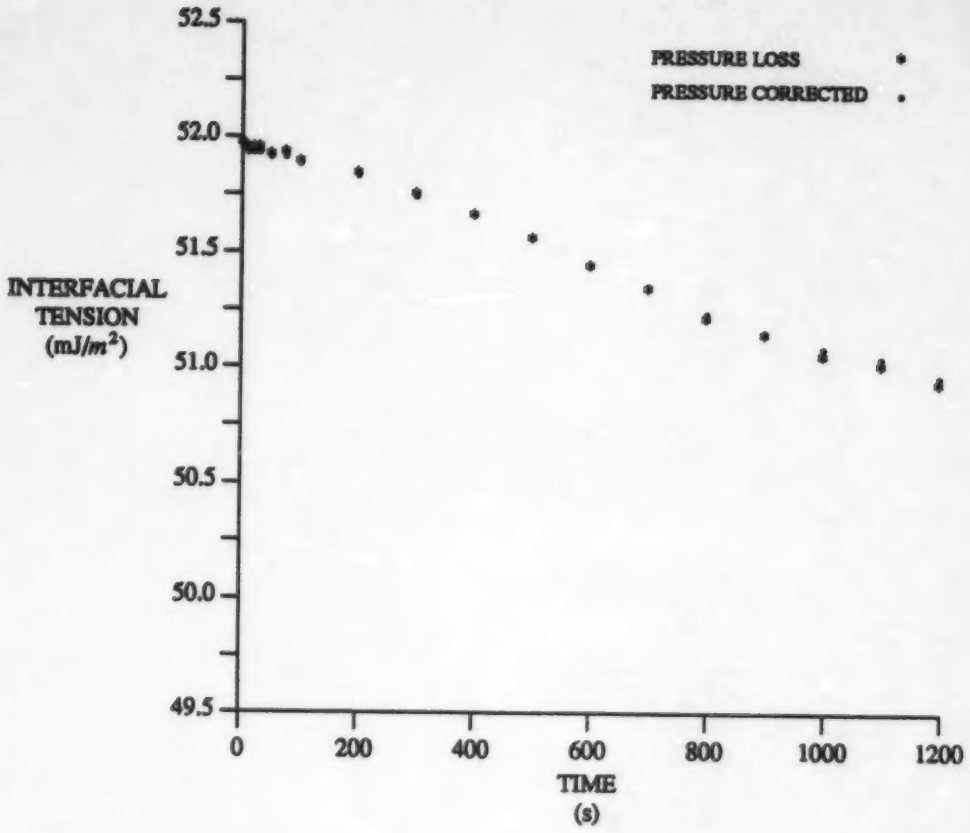

Figure 25: Interfacial tension (mJ/m^2) versus time (s) for decane in degassed doubly distilled water at 5177 psig. "*" $\Delta\rho$-value at t=0 pressure used as input for ADSA, "." $\Delta\rho$ corrected for pressure loss.

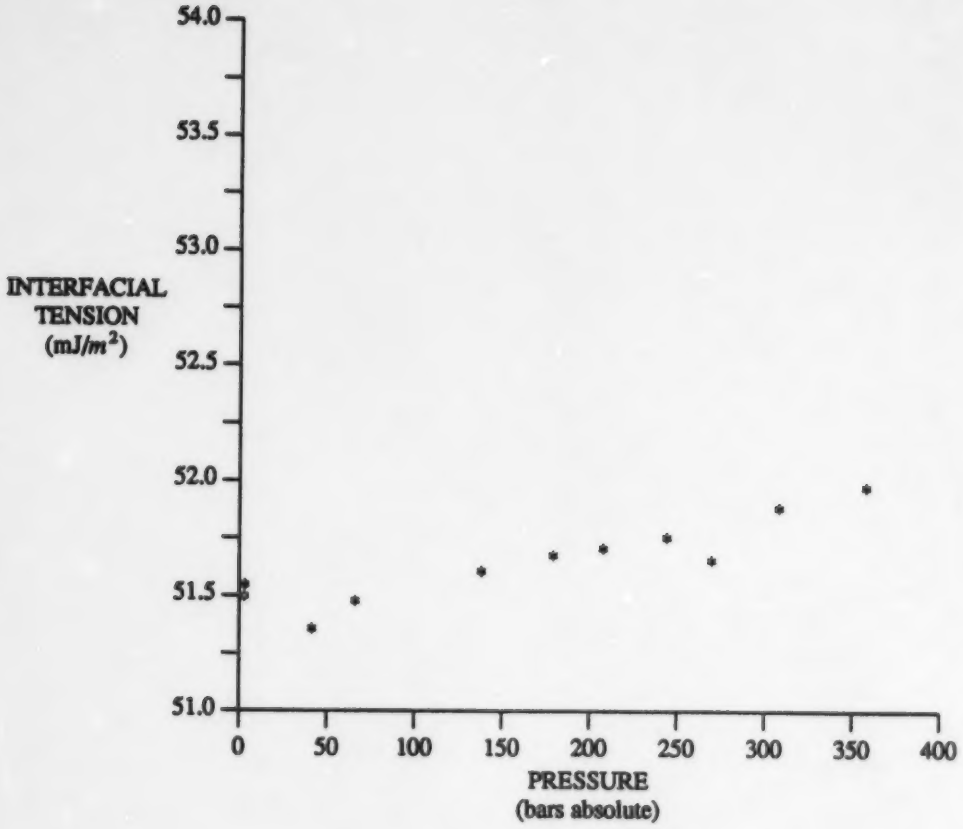

Figure 26: Interfacial tension (mJ/m^2) versus pressure (bars absolute) for decane in doubly distilled water at time t=0.

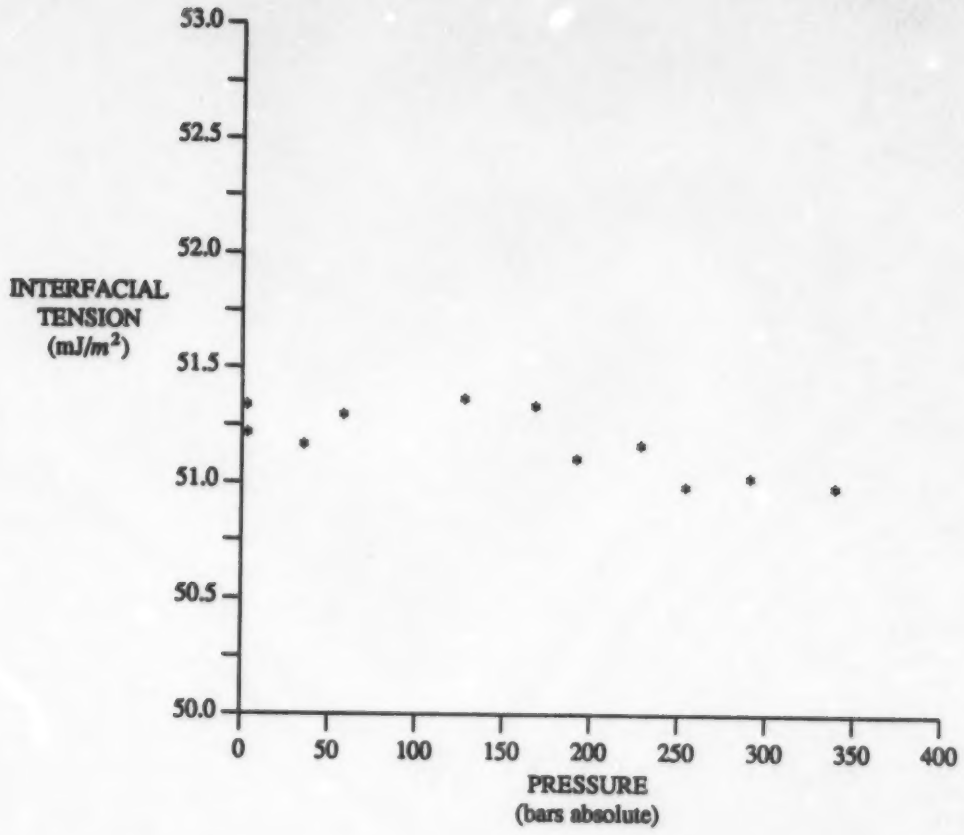

Figure 27: Interfacial tension (mJ/m^2) versus pressure (bars absolute) for decane in doubly distilled water at time t=1200.

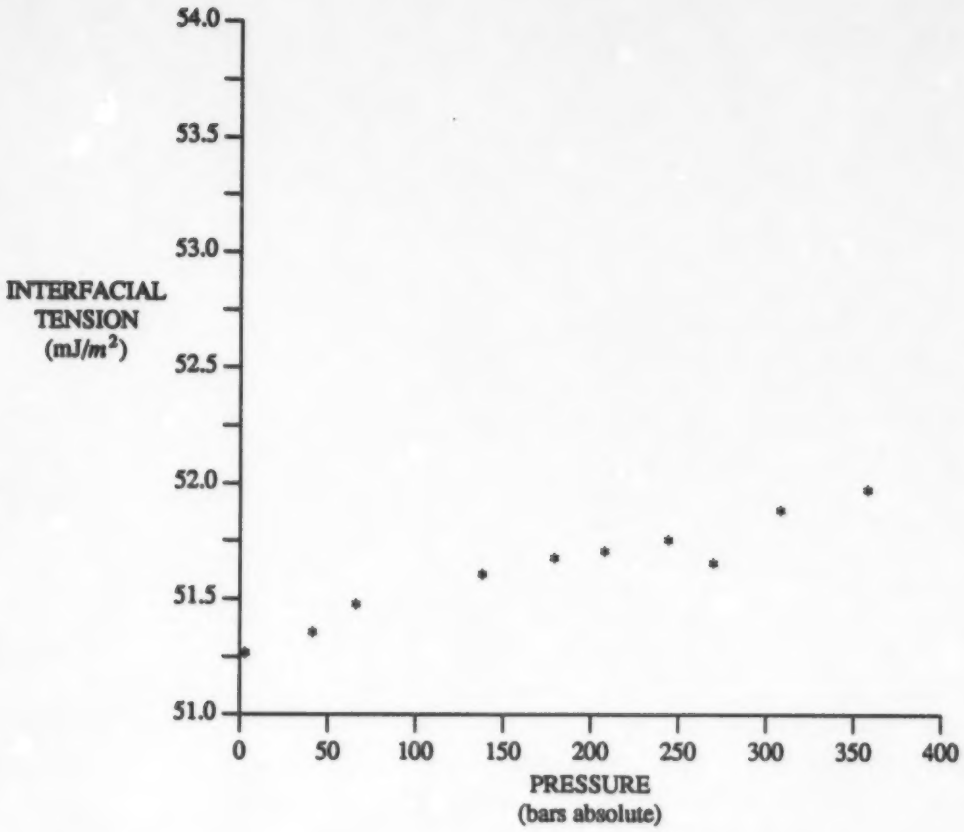

Figure 28: Interfacial tension (mJ/m^2) versus pressure (bars absolute) for decane in doubly distilled water at time t=0 for all but the first two data points which use the steady state values for γ.

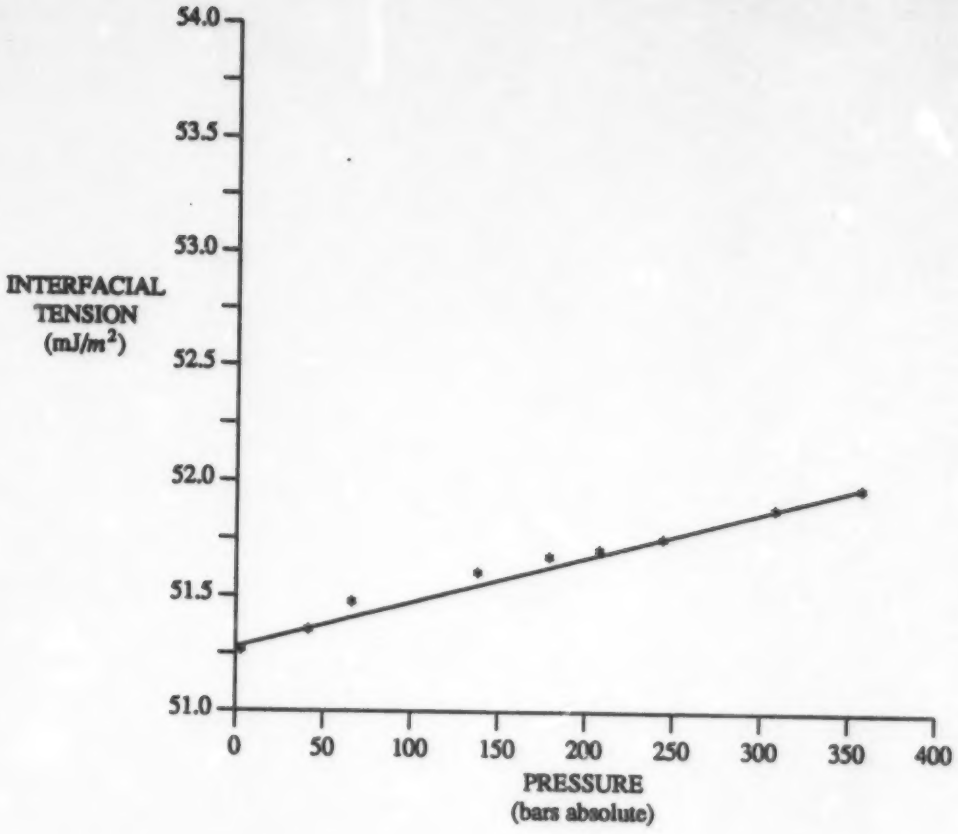

Figure 29: Interfacial tension (mJ/m^2) versus pressure (bars absolute) for decane in doubly distilled water. The solid line represents the straight line of best fit of the data.

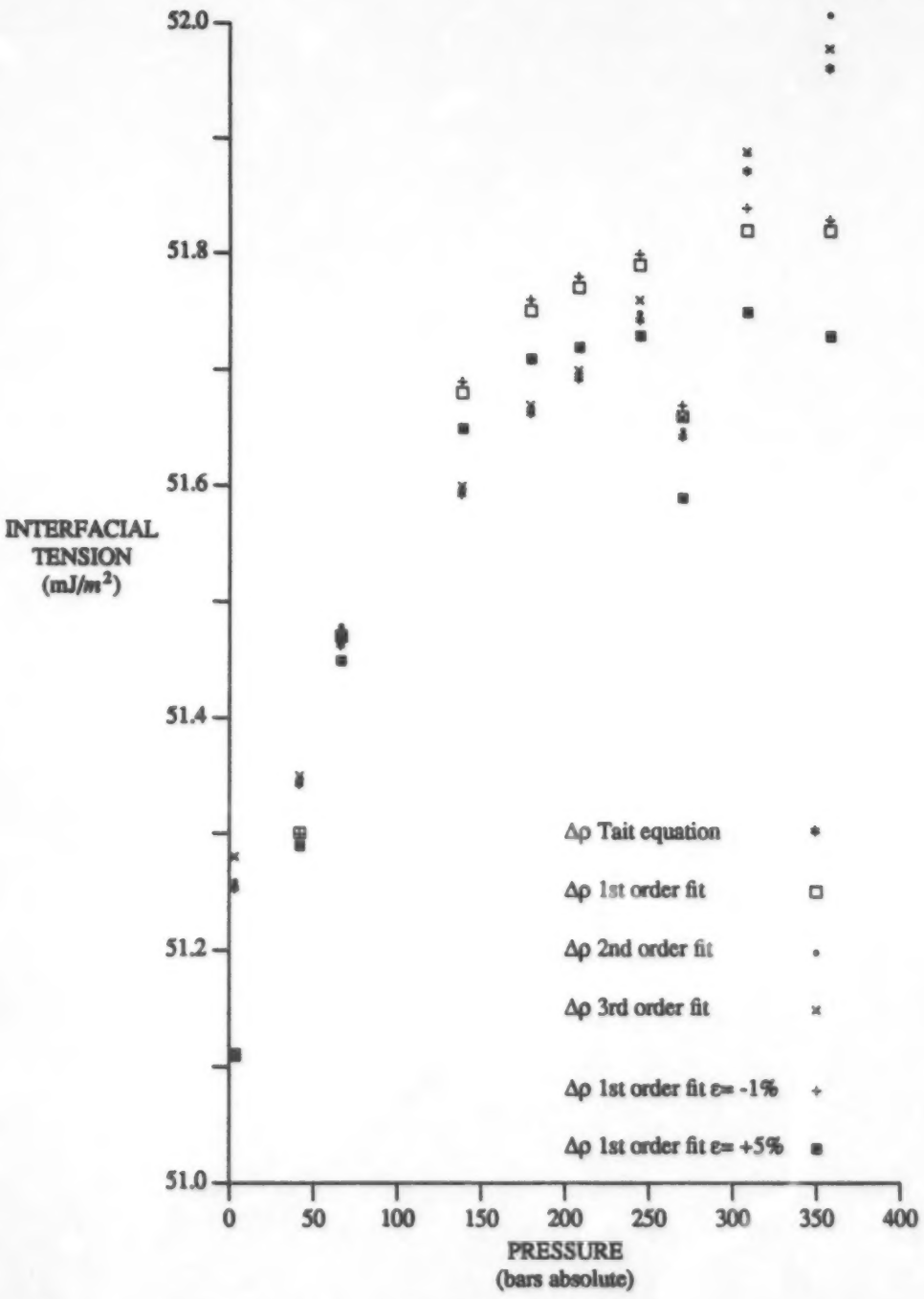

Figure 30: Interfacial tension (mJ/m^2) versus pressure (bars absolute) for decane in doubly distilled water using various equations to fit the experimental density data. These calculated Δρ values were used as input for ADSA.

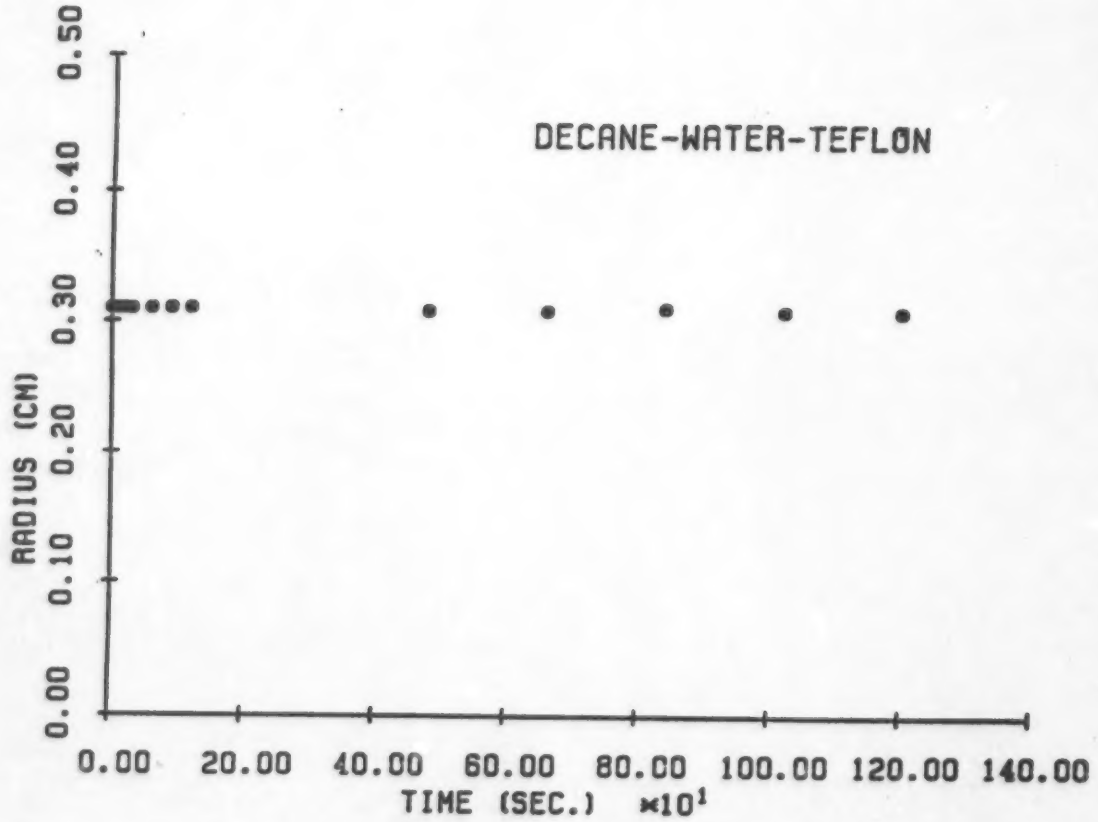

Figure 31: Radius of a water sessile drop in decane on Teflon versus time.

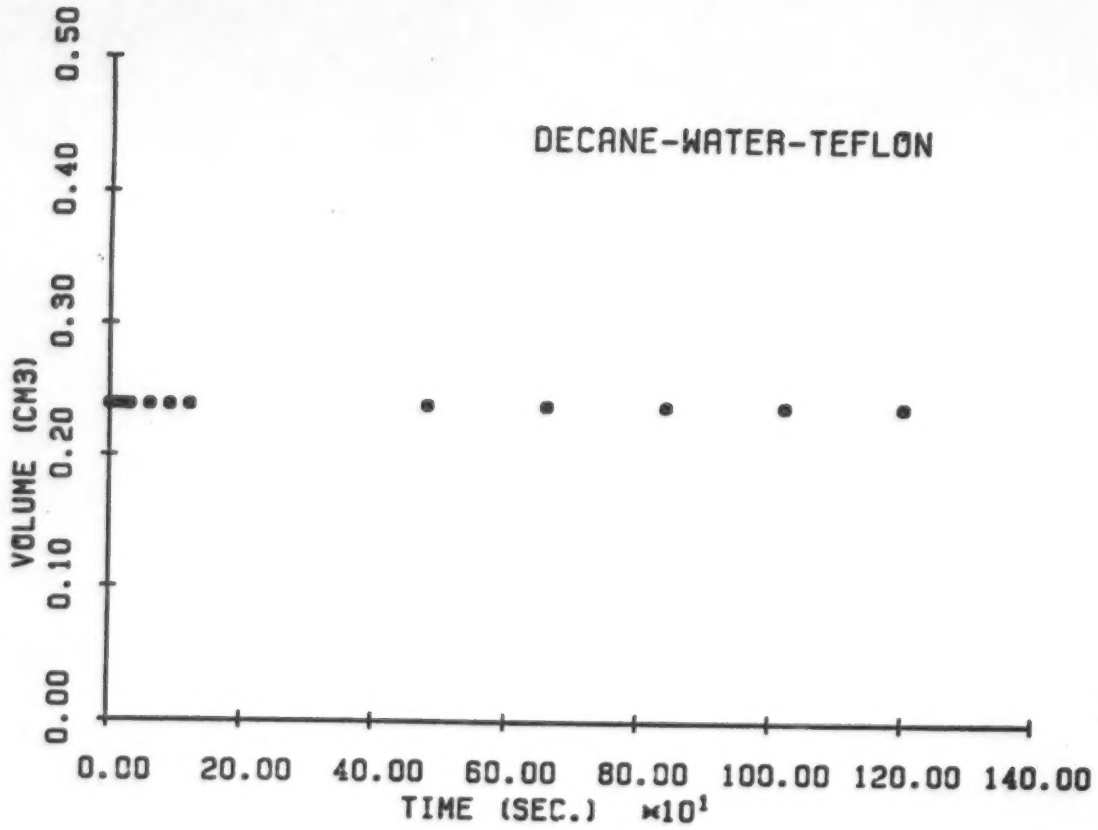

Figure 32: Volume of a water sessile drop in decane on Teflon versus time.

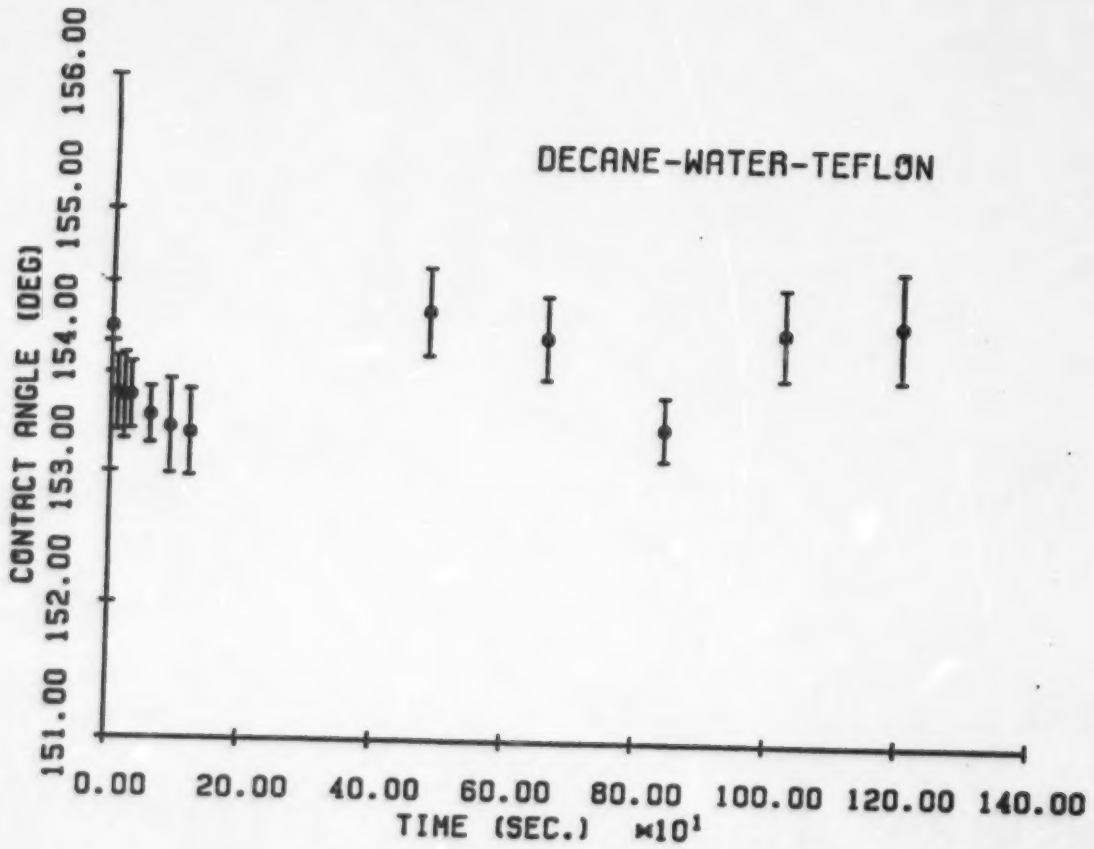

Figure 33: Contact angle of a water sessile drop in decane on Teflon versus time.

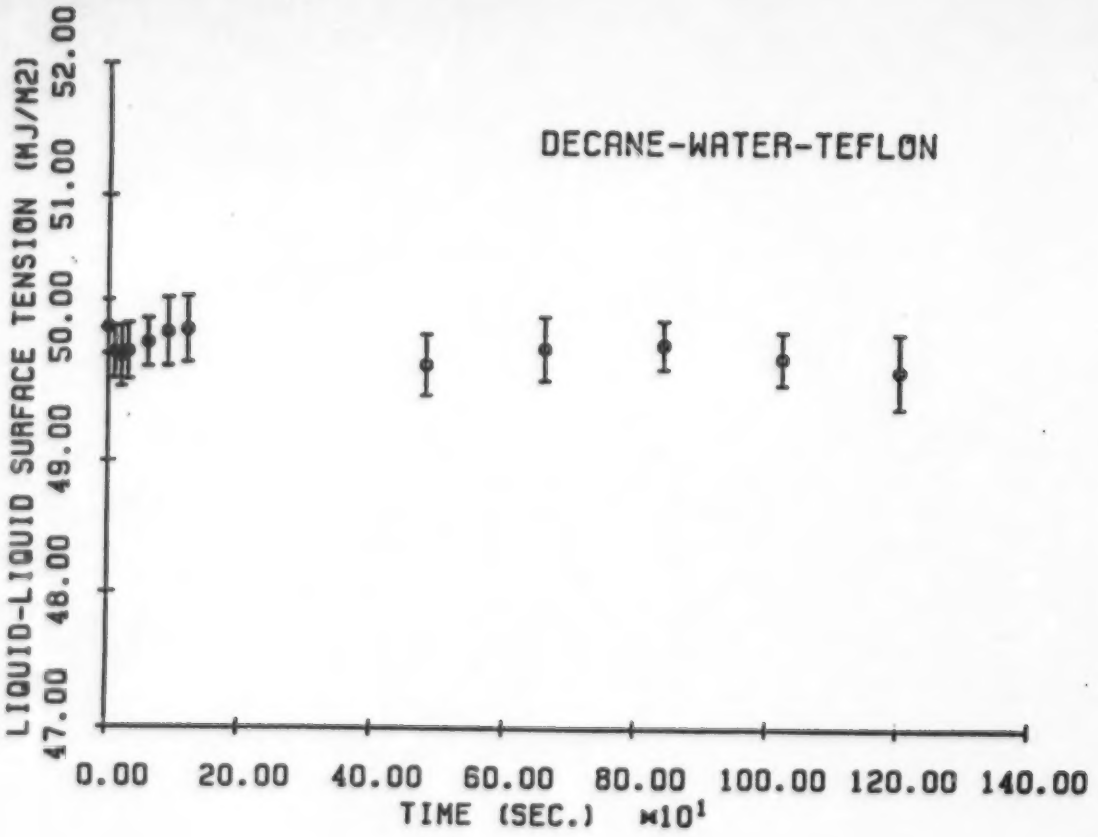

Figure 3 4: Interfacial tension of decane in water versus time measured from a sessile drop of decane in water on a Teflon substrate.

Figure 35: A laser printer reproduction of a decane sessile drop in water on a Teflon substrate.

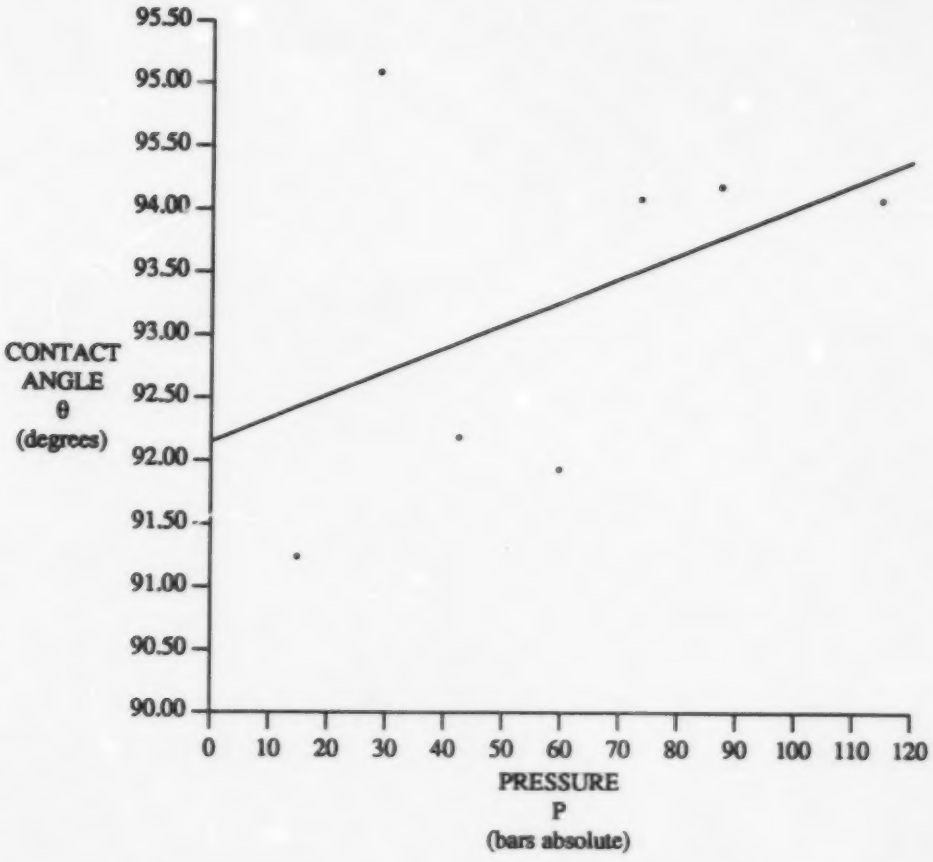

Figure 36: Contact angle θ (degrees) vs. pressure P (bars absolute) for decane in doubly distilled water.